République Algérienne Démocratique et Populaire
Ministère de l'Enseignement Supérieure et de la Recherche Scientifique

Université Echahid Hamma Lakhdar d'El-Oued

Faculté de Sciences et de La Technologies Filière: Genie Electrique

Mémoire de fin d'étude

Présenté pour l'obtention du diplôme de

MASTER ACADEMIQUE

Domaine: Sciences et Technologie

Filière: Génie électrique

Spécialité: Réseaux électrique

Réalisé par: Khennoufa Ilyas, Sahara Hossin, Miloudi Abir

Thème

Fuzzy logic maximum power point tracking MPPT techniques for photovoltaic systems

Devant le jury composé de:		
Dr.Serhoud Hicham	Université Echahid Hamma Lakhdar	Président
Dr.Kaid Imad Eddine	Université Echahid Hamma Lakhdar	Examinateur
Dr. Djaafar Toumi	Université Echahid Hamma Lakhdar	Encadreur

2023-2024

بسم الله الرحمن الرحيم

الشكر والعرفان

قال تعالى: "رب أوزعني أن أشكر نعمتك التي أنعمت عليّ وعلى والدي وأن أعمل صالحا ترضاه وأدخلني برحمتك في عبادك الصالحين."

نحمد الله أولا وأخيرا ونشكره شكراً يليق بعظمته وجلاله أن يسر لنا إتمام هذا العمل فله الحمد والثناء والمنه.

من مبدأ التقدير والاعتراف بالجميل نتوجه بالشكر مع خالص تقديرنا واحترامنا إلى أستاذنا ومشرفنا الفاضل "الدكتور: تومي جعفر" على ما أبداه من سعة صدر وصبر وتحمل ومن نصح وإرشاد ونسأل الله العلي العظيم أن يجعل ذلك في ميزان حسناته.

كما نتوجه بالشكر الممزوج بالحب إلى الوالدين الكريمين لأنهما كانا العون لنا لإكمال مسيرتنا الدراسية.

كما نتقدم بالشكر الجزيل إلى كل الأساتذة.

وكما نتقدم بالشكر إلى عمال كلية التكنولوجيا وإلى الزملاء والزميلات.

والشكر موصول لأعضاء اللجنة الموقرة على قبولهم مناقشة هذا العمل.

وفي الأخير نرجو أن ينال جهدنا هذا القبول، وحسبنا أننا اجتهدنا والكمال لله وحده عز وجل.

الإهداء

إلى من عاش فينا قبل ان نعيش فيه، و عرفناه في دفاتر التضحيات، إلى وطننا الثاني فلسطين، قبلتنا الاولى ومسرى نبينا الكريم. جمعنا الله في أقصاها فاتحين مهللين مكبرين، و ما ذلك على الله بعسير.

مثل كل البدايات لا تتم إلا بتسيره و ما بلغنا النهايات إلا بتوفيقه و ما حققنا المراد إلا بفضله فالحمد لله الذي وفقنا لإتمام هذه الخطوة في مسيرتنا التعليمية .

*أهدي عملي هذا إلى من كان دعائها سر نجاحي **أمي** الحبيبة*

*إلى من ذكراه لا تفارقني **أبي** – رحمك الله –*

*إلى **اخوتي** الاعزاء حفظهم الله*

*إلى الأستاذ المشرف : **تومي جعفر***

إلى من أحبهم ويحبوني أهدي ثمرة جهدي

ميلودي عبير

الإهداء

الحمد لله الذي وفقنا لهذا وما كنا لنصل إليه لولا فضله علينا أما بعد

أهدي هذا العمل المتواضع إلى **أمي** و **أبي** العزيزين حفظهما الله

وإلى أفراد أسرتي ، سندي في الدنيا **ولا** أحصي لهم فضل

إلى الأستاذ المشرف : **تومي جعفر**

إلى كل أقاربي و إلى كل الأصدقاء و الأحباب من دون استثناء

إلى أساتذتي الكرام و كل رفقاء الدراسة

إلى كل من كان النجاح طريقه والتفوق هدفه والتميز سبيله

و في الأخير أرجوا من الله تعالى أن يجعل عملنا هذا نفعا يستفيد منه جميع

الطلبة المتربصين المقبلين على التّخرج .

خنوفه إلياس

الإهداء

إلهي، ليس بسبب جهودي واجتهادي، بل بسبب عونك وكرمك ونعمتك، لك مني خالص الحمد والشكر.

أهدي شهادتي لمن منحني حياته، لمن أوكلت أمره إلى الله .... **والدي**

وإلى جنتي في الحياة، إلى شعور الحب وشعور الحنان، إلى الظل الذي أعيش فيه .... **أمي**

إلى أفضل الداعمين والأحبة .... **إخوتي**

وكل شكري وامتناني لمن لا أستطيع إحصاء لطفهم، لمن شجعني وساندني

وأشكر أستاذي المشرف الذي بذل كل جهوده في إعداد هذه المذكرة وكان معنا في كل الأوقات، وكل الكلمات لا تكفي

لشكر الدكتور **تومي جعفر**.

سحارة حسين

الملخص

يقدم هذا البحث محاكاة المصفوفة الكهروضوئية لتتبع نقطة الذروة **(MPPT)** باستخدام التحكم المنطقي المضبب. ولذلك، يتم إجراء المحاكاة في الوقت الحقيقي في **MATLAB/Simulink** استنادًا إلى النموذج الكهروضوئي ومحول التعزيز والتتبع القائم على المنطق الغامض. أجريت دراسة مقارنة ضد متحكم الاضطراب والمراقبة **.(P&O)** يمكن لجهاز التتبع المعتمد على تقنية المنطق الغامض أن يتتبع بنجاح نقطة الطاقة القصوى بسرعة كبيرة ولديه تحكم دقيق عند مقارنته بـ **P&O.** وبشكل عام نستنتج أن **MPPT**باستخدام تقنية المنطق الضبابي يأخذ استجابة سريعة ويمكن أن يحسن أداء النظام الكهروضوئي**.**

الكلمات المفتاحية : النظام الكهروضوئي ملاحقة نقطة الاستطاعة الأعظمية (MPPT) ، المتحكم الضبابي، المبدل المستمر الخافض للجهد، معدل عرض نبضات PWM.

Abstract

This research introduces the simulation of PV array to track the peak point (MPPT) using fuzzy logic control. Therefore, real time simulation is performed in MATLAB/Simulink based on a PV model, boost converter and fuzzy logic based tracker. A comparative study is carried out against perturb and observe (P&O) controller. The fuzzy logic technique based tracker can successfully track the maximum power point very fast and has precise control when compared to the P&O. The overall we conclude that the MPPT using the fuzzy logic technique takes a fast response and can improve the performance of the PV system.

Key words: photovoltaic System, Maximum Power Point Tracking (MPPT),Fuzzy Logic Controller, Buck Converter, Pulse Wide Modulation(PWM).

Résume

Cette recherche introduit la simulation d'un générateur photovoltaïque pour suivre le point de crête (MPPT) à l'aide d'un contrôle de logique floue. Par conséquent, une simulation en temps réel est effectuée dans MATLAB/Simulink sur la base d'un modèle PV, d'un convertisseur élévateur et d'un tracker basé sur la logique floue. Une étude comparative est réalisée avec un contrôleur perturber et observer (P&O). Le tracker basé sur la technique de logique floue peut suivre avec succès le point de puissance maximale très rapidement et dispose d'un contrôle précis par rapport au P&O. Dans l'ensemble, nous concluons que le MPPT utilisant la technique de logique floue répond rapidement et peut améliorer les performances du système photovoltaïque.

Mots-clés : système photovoltaïque, suivi du point de puissance maximale (MPPT), contrôleur flou, convertisseur abaisseur de tension DC-DC, modulation de largeur d'impulsion (PWM).

Sommaire

General Introduction

Chapter I: Photovoltaic generalities

Chapter II: Modeling of photovoltaic system

Chapter III: Pursuit of the maximum power point

Chapter IV: Results and simulation

Général conclusion

Bibliographic références

List of figure

List of table

List of Abbreviations

المعنى باللغة العربية	المعنى باللغة الانجليزية	الإختصارات
أمبير	Ampere	**A**
محول تشابهي رقمي	Analog to Digital Converter	**ADC**
مركز الجاذبية	Center Of Gravity	**COG**
تغير الخطأ	Change in error	**CE**
التيار المستمر	Direct Current	**DC**
الخوارزميات التطورية	Evolutionary Algorithms	**EA**
الخطأ	Error	**E**
هرتز	Hertz	**Hz**
نقطة الإستطاعة الأعظمية	Maximum Power Point	**MPP**
ملاحقة نقطة الإستطاعة الأعظمية	Maximum Power Point Tracking	**MPPT**
ميلي ثانية	Millesecond	**Ms**
الإضطراب والمراقبة	Perturb and Observe	**P&O**
معدل عرض النبضة	Pulse Width Modulation	**PWM**
فولت	Voltage	**V**
واط	Watt	**W**

Général Introduction

General Introduction

This document provides a -ne, polycrystalline, and amorphous silicon are explained in terms of their structure, operating principles, and efficiency ranges.

The modeling aspects of PV cells and systems are then covered in detail. Equivalent circuit models are presented that can accurately represent the current-voltage characteristics of a single PV cell as well as an entire PV generator composed of series/parallel connected cells. The influence of various parameters like solar irradiance levels, cell temperature, series resistance, parallel resistance and ideality factors on the I-V curve is methodically analyzed. Modeling equations are derived to calculate these parameters from manufacturer datasheet values.

A critical aspect discussed is maximum power point tracking (MPPT) required to continuously extract the maximum available power from a PV generator as environmental conditions change. The document evaluates different options starting with a simple direct coupling between the PV generator and load. However, this does not ensure maximum power transfer. DC-DC converters, specifically the boost converter topology, are introduced as an interfacing stage between the PV generator and load .

To control the duty cycle of these DC-DC converters and ensure operation at the maximum power point, several MPPT algorithms are studied. These include the widely used perturb and observe (P&O) technique, variants using fuzzy logic to improve tracking performance, as well as a fuzzy logic based MPPT controller designed completely using fuzzy reasoning concepts like fuzzification, inference rules and defuzzification. The pros and cons of each algorithm are discussed.

Overall, this document presents a systematic approach to understanding, modeling and controlling PV systems to enable efficient conversion of solar energy into electricity by continuously operating at the maximum power point despite variations in solar irradiance, temperature and loading conditions.

CHAPITRE I

Photovoltaic generalities

Photovoltaic generalities

I.1. Introduction:

The sun is an almost inexhaustible source of energy sent to the surface of the earth, the annual radiation represents approximately 15,000 times the energy consumption of humanity. This corresponds to an instantaneous power received of 1 kilowatt peak per square meter (kWc/m²) distributed over the entire spectrum, from ultraviolet to infrared. The deserts of our planet receive more energy from the sun in 6 hours than humanity consumes in a day [1].

For a very long time, man has sought to exploit the energy emitted by the sun. Most uses are direct, such as in agriculture, through photosynthesis or in various drying and heating applications, both artisanal and industrial. This energy is available in abundance across the entire earth's surface; despite significant attenuation when passing through the atmosphere, a significant quantity still reaches the surface of the earth. We can thus count on 1000 W/m² in temperate zones and up to 1400 W/m² when the atmosphere is lightly polluted by dust or humidity. The solar flux received at ground level therefore depends on several parameters such as:

- The orientation, nature and inclination of the earth's surface
- The latitude of the collection location, its degree of pollution as well as its altitude
- The time of year
- The moment considered during the day
- The nature of cloud layers

The most favorable areas are listed in the form of an atlas and highlight “solar deposits” on the earth's surface [2].

I.2. The solar spectrum:

The spectrum of solar electromagnetic radiation covers a very wide range, from radio radiation to X-rays. We generally distinguish the continuous spectrum, which is approximately that of a black body at around 6000°K, and the real spectrum emission from the sun [3].

Figure I.1 shows the black body energy curve at 6000K, solar radiation outside the atmosphere and solar radiation at sea level as a function of wavelength. These curves show that 9.2% of the energy in this spectrum is found in the ultraviolet, 42.4% in the visible and 48.4% in the infrared.

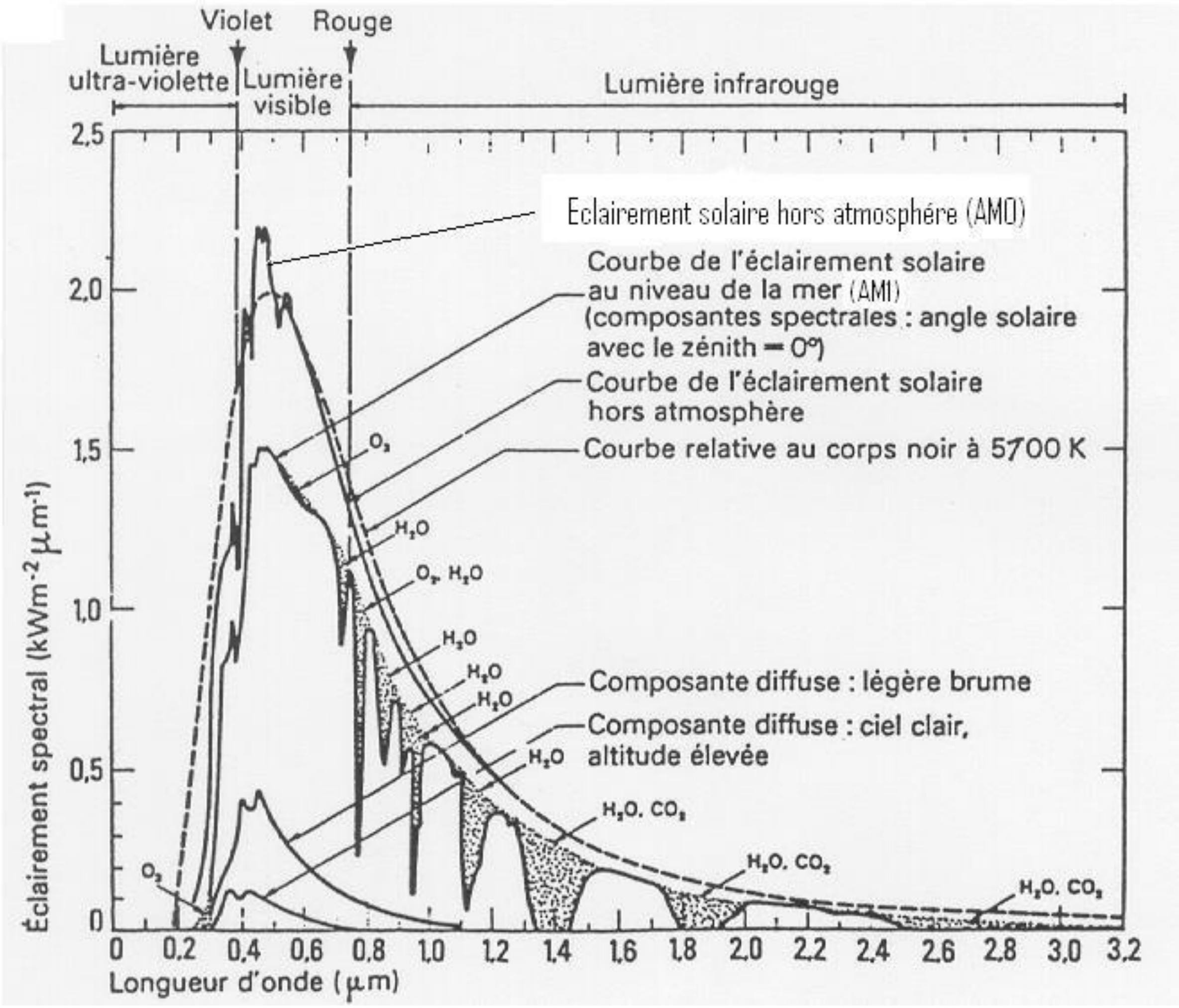

Figure I.1: Solar illumination [4].

From Figure I-1 we see that solar radiation can be reflected, scattered or absorbed. Furthermore, the spectra of reflected, scattered, and absorbed radiation are different.

On the earth's surface, the solar spectrum is not the same as in space, because it is reduced by the absorption of molecules present in the atmosphere (O3, CO3, H2O). Weather conditions as well as the presence of micro particles volatilized in the atmosphere.

I.3. Duality of light:

Light can be considered in the form of electromagnetic waves of wavelength λ or in the form of photons, corpuscles having an energy E linked to λ by the following relationship. [5]

$$E = h\,.\,v = \frac{h.c}{\lambda} \tag{I-1}$$

With: h: Planck's constant (j)

c: speed of light in a vacuum (m)

v: frequency (s^{-1})

λ: wavelength (m)

The notion of wave/particle duality is important for understanding the phenomena of interaction between radiation and a material.

The wavelengths of terrestrial solar radiation are between 0.2µm (ultraviolet) and 4µm (infrared) with a maximum energy at 0.5µm. 97.5% of solar energy is between 0.2µm and 2.5µm. From 0.4µm to 0.78µm, the spectrum corresponds to the visible region. Solar energy sensors must therefore be compatible with these wavelengths to be able to trap photons and release them in the form of heat or electrons.

Table I.1 gives the characteristic energy values of photons for various wavelengths, as well as the corresponding areas of the light spectrum [6].

λ (µm)	**E(ev)**	**Area**
0.2	6.2	Ultraviolet
0.4	3.1	Visible blue
0.5	2.48	Visible yellow-green
0.78	1.59	Visible yellow-green
1	1.24	Infrared
2	0.62	Infrared
4	0.31	Infrared

Table I.1: Energy values of photons from the solar spectrum.

For solar radiation to produce an electric current in a given material, thus acting as a sensor, the photons must first be absorbed by one or more materials sensitive to the wavelength of the photons. Then, the energy of the photons excites electrons, which are then collected to form a global electric current.

I.4. Solar radiation:

The radiation emitted by the sun is made up of electromagnetic waves, part of which constantly reaches the upper limit of the Earth's atmosphere. Due to the surface temperature of the sun (around 5800 K), this electromagnetic radiation is in the wavelength range of visible light (between 0.4 and 0.75 µm) and in the near infrared (at-beyond 0.75 and up to approximately 4 µm). The energy carried by this radiation, averaged over a year and over the entire upper limit of the atmosphere, corresponds to an illumination of 340 Wm^{-2} (Figure I.5). An energy balance shows that, of this quantity of illumination brought by the sun to the earth + atmosphere system, approximately 100 Wm^{-2} are reflected towards space, only the rest is absorbed, one third by the atmosphere and two thirds by the earth's surface [5,18].

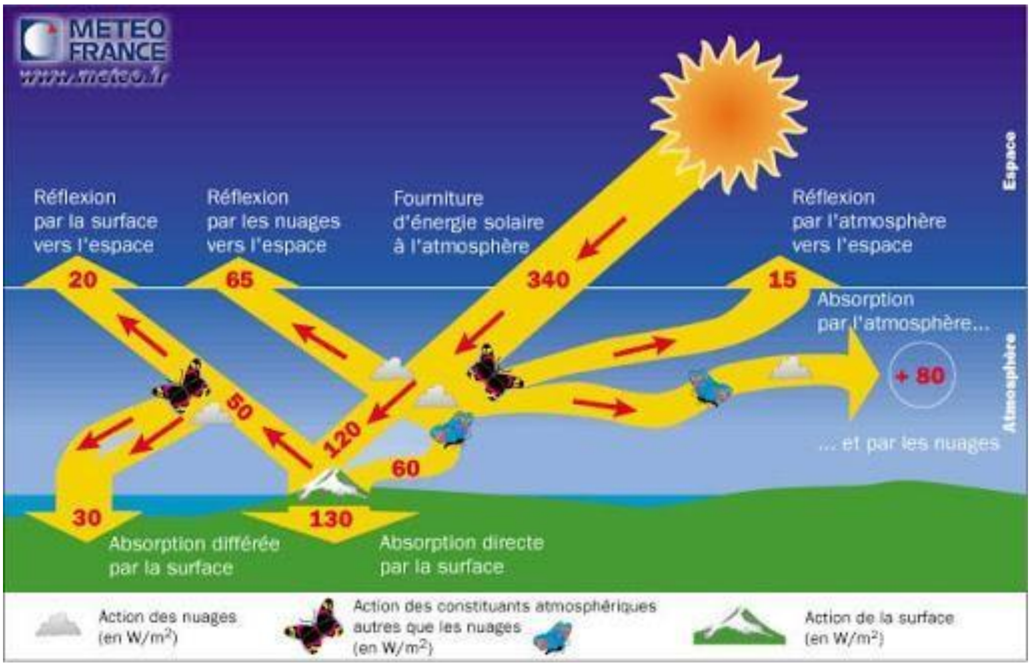

Figure I.2: Solar radiation transmitted to the earth.

Figure I.5, published by Météo France, shows that nearly a quarter of this incident lighting is reflected in space by the atmosphere: such reflection is essentially due to clouds (65 Wm^{-2}), the rest (15 Wm^{-2}) being due to other atmospheric constituents such as gases and aerosols. This leaves (180 Wm^{-2}) which reach the earth's surface at the end of a transmission, two-thirds of which (120 Wm^{-2}) takes place directly, the rest (60 Wm^{-2}) taking place by downward diffusion. [7]

A complex process of interaction between downward diffusion and reflection then occurs. Of the 180 Wm^{-2} incidents, the earth's surface, which has a high average albedo, should return approximately 50 Wm^{-2} to the atmosphere. In fact, most of the illumination it thus reflects returns to it sooner or later and is partially added to the 180-50 =130 W$m^{-2}$of solar radiation not reflected in its contact. Although the absorption of solar radiation is a continuous phenomenon, we can simplify the understanding of the preceding process by assuming that the 50 Wm^{-2}reflected by the surface of the globe are distributed between 20 Wm^{-2} definitively returned towards the interplanetary space and 30 W. m−2 which return to the earth's surface after delayed diffusion downwards. This energy is added to the 130 Wm^{-2} initially not reflected to constitute approximately the 160 Wm^{-2} absorbed by the earth's surface [7].

I.5. Different types of radiation:

As it passes through the atmosphere, solar radiation is absorbed and scattered. On the ground, we can distinguish several components.

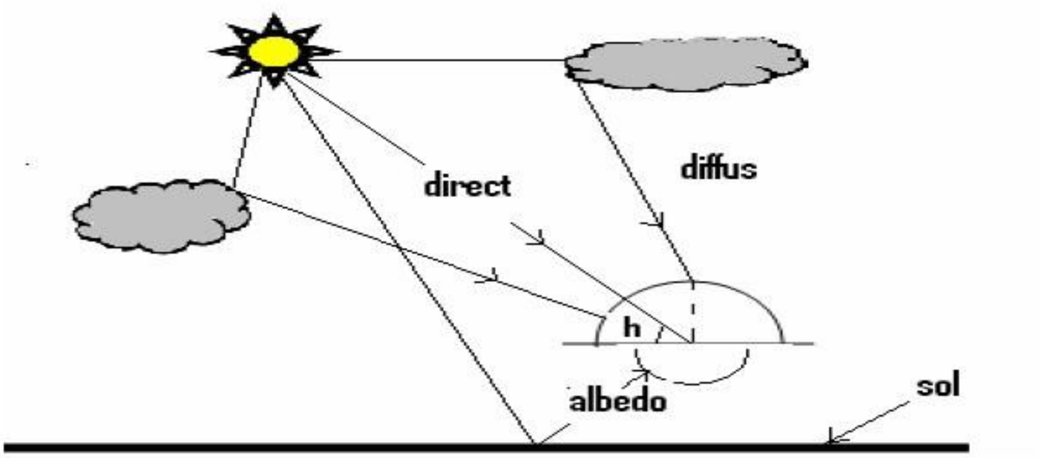

Figure I.3: Different radiation components.

I.5.1. Direct radiation:

Direct radiation is radiation received directly from the Sun. It can be measured by a pyrheliometer.

The direct radiation received in the plane of the sensor is:

$$I(\alpha.\gamma) = I.\cos(i) \quad \text{(I-2)}$$

With: I: normal direct radiation

i: (Angle of incidence): it is the angle between the direction of the sun and the normal to the plane [8].

I.5.2. Diffuse radiation:

Diffuse radiation results from the diffraction of light by atmospheric molecules, and from its refraction by the ground, it reaches the entire sky [9].

Diffuse radiation (Dh) is the radiation emitted by obstacles (clouds, ground, buildings) and comes from all directions. It can be measured by a pyranometer with a screen hiding the sun [10].

In the sensor plane the diffuse radiation is given by [11]:

$$D_{(\alpha,\gamma)} = \left(\frac{1+\cos(\alpha)}{2}\right).D_h + \boldsymbol{Alb}.\left(\frac{1-\cos(\alpha)}{2}\right).G_h \quad \text{(I-3)}$$

With : $\boldsymbol{Alb}$: albedo (ground reflection coefficient)

h: sun height [degree]

D_h: Diffuse on horizontal plane

G_h: Global horizontal

For a vertical plane ⇒ Dv = 0,5 . ($Hh + \alpha \cdot Gh$) (I-4)

I.5.3. Albedo or Reflected:

It is the fraction of incident radiation scattered or reflected by an obstacle. This term being generally reserved for the ground and clouds, it is an average value of their reflector for the radiation considered, and for all possible angles of incidence. By definition, the black body has zero albedo.

$$\text{Albedo } (\boldsymbol{Alb}) = \frac{reflected\ energy}{energy\ received} \quad \text{(I-5)}$$

I.5.4. Global radiation:

The overall radiation on the ground therefore depends on the composition and thickness of the atmosphere crossed by the light rays during the day. It is broken down into direct radiation and diffuse radiation, and it is these two radiations which are exploited by solar generators [12].

In the case of a horizontal surface, the overall radiation is written:

$$G = I.\sin(h) + D_h \quad \text{(I-6)}$$

For any plane, the global radiation is:

$$G_{(\alpha,\gamma)} = I_h.\frac{\cos(\mathrm{i})}{\sin(h)} + \frac{D_h}{2}.\left[1 + \cos\left(\frac{\pi}{2} - \gamma\right)\right] + \frac{D_h}{2}.\boldsymbol{Alb}.\left[\mathbf{1} - \boldsymbol{cos}\left(\frac{\boldsymbol{\pi}}{\mathbf{2}} - \gamma\right)\right] \quad \text{(I.7)}$$

With: I_h: Direct horizontal

I.6. Solar potential in Algeria:

Solar potential is the total amount of solar energy irradiation received on a given region surface over time in a specific location. In Algeria, the potential is the greatest in the entire Mediterranean basin:

- 1169,440 TWh/year
- 5,000 times Algerian electricity consumption
- 60 times the consumption of the Europe of 15 (estimated at 3,000 TWh/year). Average energy received in KWh/m²/year:
- Coastal regions 1700
- Highlands 1900
- Sahara 2650

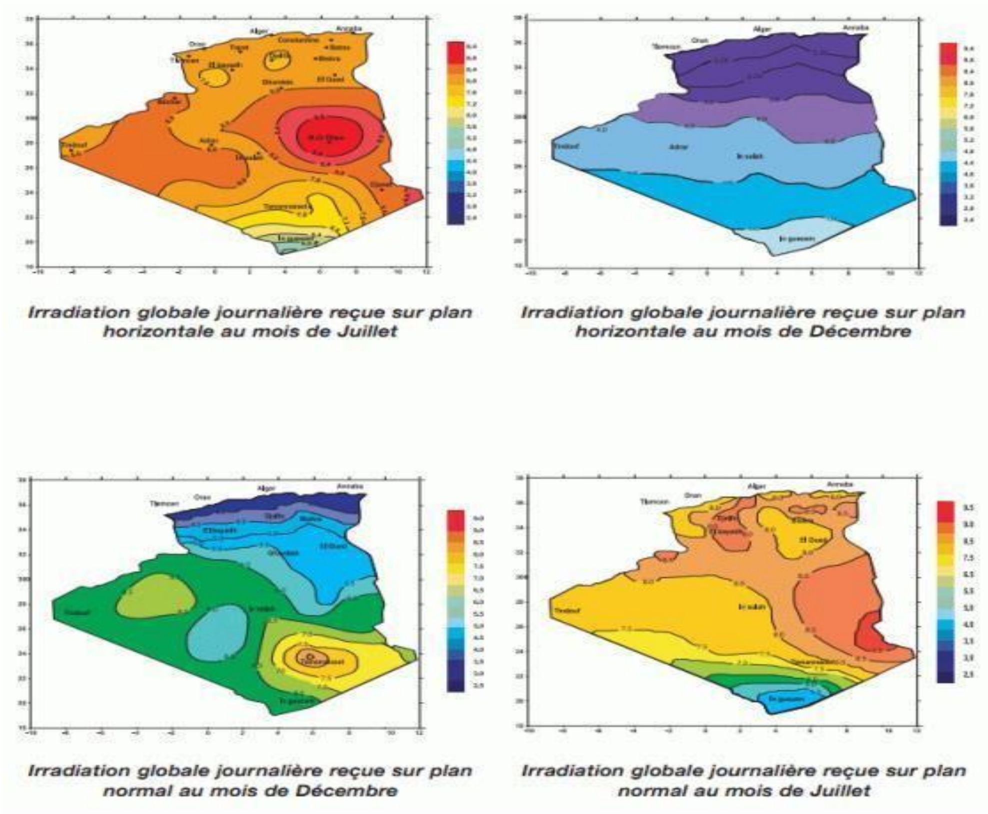

Figure I.4: Solar potential in Algeria [13].

I.7. Photovoltaic solar energy:

The term "photovoltaic", often abbreviated by the acronym "PV", was formed from two words "photo", a Greek word meaning light and "Volta", the name of the Italian physicist Alessandro Volta who invented the electric battery in 1800 [14].

Photovoltaic solar energy comes from the direct conversion of energy from photons, included in solar radiation, into electrical energy through sensors made with materials sensitive to visible wavelengths [15].

I.7.1. The photovoltaic cell:

The photovoltaic cell or solar cell is the smallest element of a photovoltaic installation. It is made of semiconductor materials and directly transforms light energy into electrical energy.

Photovoltaic cells are made up of:

- A thin semiconductor layer (material with a band gap, which acts as an energy barrier that electrons cannot cross without external excitation, and whose electrical properties can be varied) such as silicon, which is a material with relatively good conductivity.
- An anti-reflective layer allowing maximum penetration of solar rays
- A conductive grid on the top or cathode and a conductive metal on the bottom or anode.

The most recent ones even have a new combination of reflective multilayer just below the semiconductor, allowing light to bounce longer within it to improve efficiency.

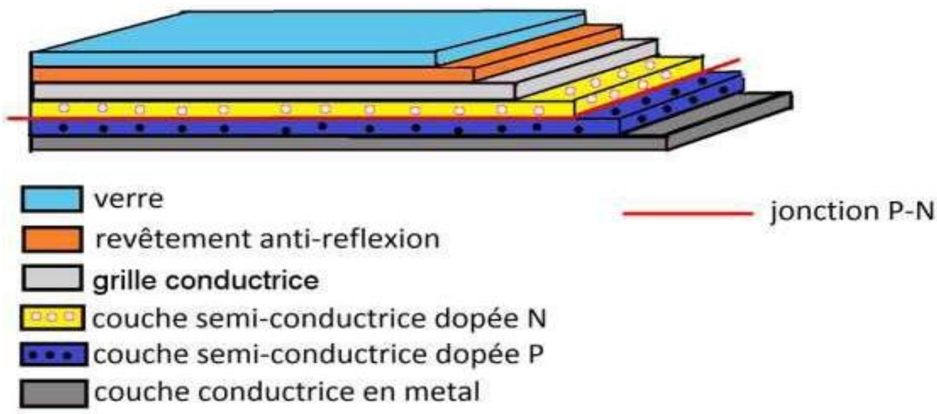

Figure I.5:basic structure of a solar cell.

A photovoltaic cell is based on the physical phenomenon called photovoltaic effect which consists of establishing an electromotive force when the surface of this cell is exposed to light. The voltage generated can vary between 0.3V and 0.7V depending on the material used and its arrangement as well as the temperature and aging of the Cell. [16]

I.7.2. Photovoltaic conversion:

a) **Semiconductor**

Semiconductor materials are bodies whose electrical resistivity is intermediate between that of conductors and that of insulators. The four valence electrons of silicon make it possible to form four covalent bonds with a neighboring atom. In this case, all electrons are used and none are available to create an electric current. [17]

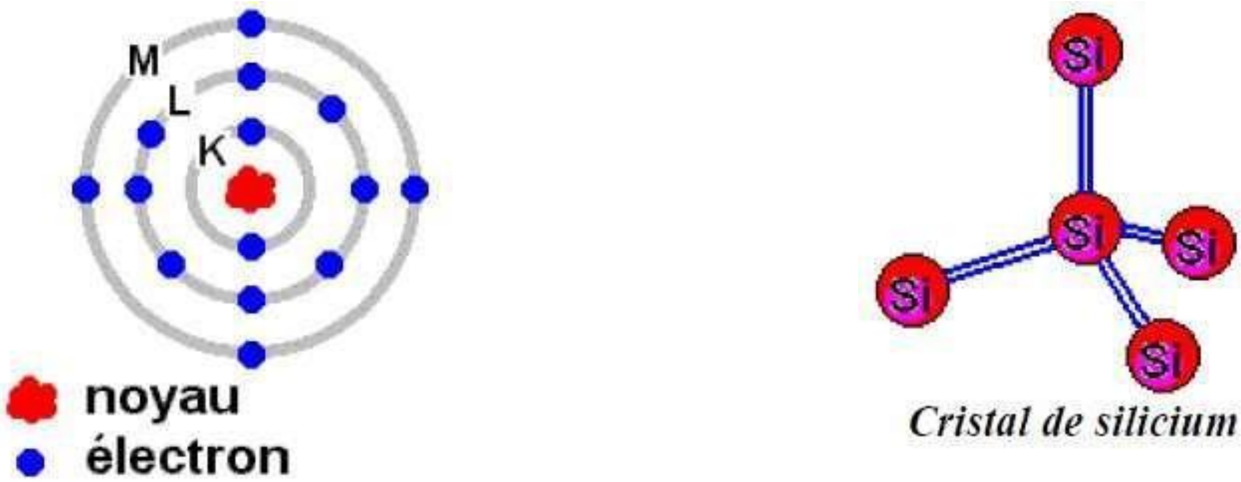

Figure I.6: Atomic presentation of the semiconductor (silicon).

b) **Semiconductor doping**

To increase the conductivity of semiconductors, impurities are introduced. This process is called doping. i. N-type doping

We replace a silicon atom with a pentavalent atom (phosphorus p). Four of them provide connections with neighboring silicon atoms and the fifth remains available; it will be excited towards the conduction band very easily by thermal agitation.

Hence the number of free electrons will increase significantly: in this case the number of holes is much lower than the number of free electrons. We thus obtain an N (negative) doped crystal. [17]

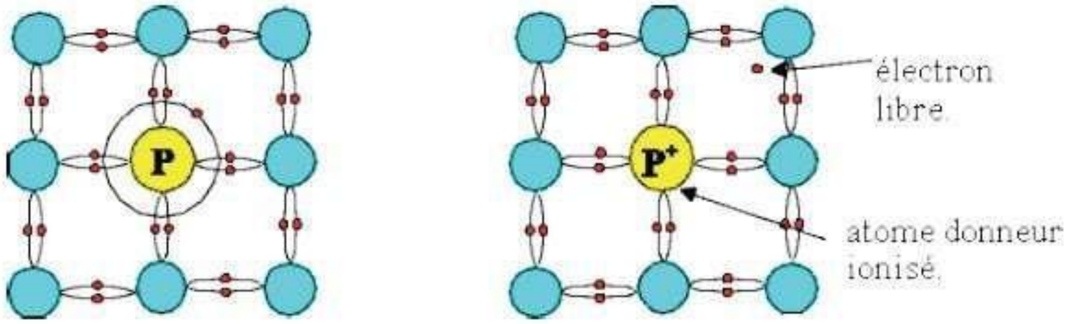

Figure I.7:n-type semiconductor doping. [17]

c) P-type doping

In the same way we introduce trivalent atoms, its three electrons will ensure covalent bonds with three neighboring atoms but leave a hole in the fourth. This hole moves step by step in the crystal to create a current.

Here the number of holes is much greater than the number of free electrons of the intrinsic crystal, we therefore obtain a P-doped crystal (positive), the impurities used are often Boron B. [17]

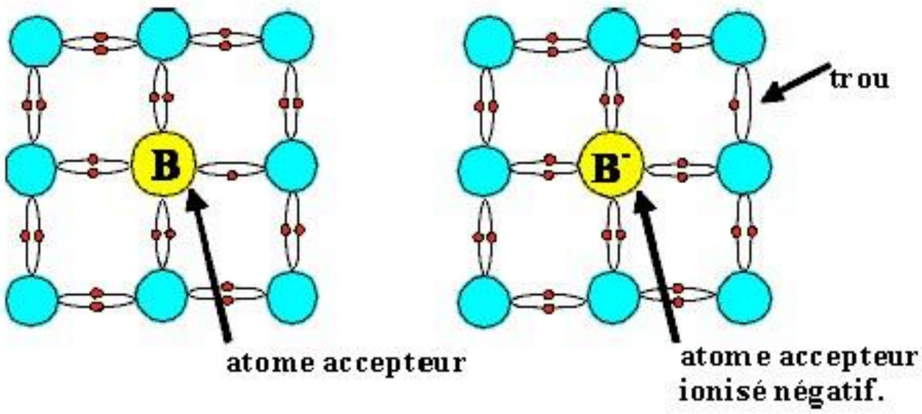

Figure I.8: p-type semiconductor doping. [17]

d) The PN Junction

A PN junction is the joining of a P-doped region and an N-doped region. During this assembly the free charge carriers attract each other and recombine in the junction zone where the free carriers disappear: this is the transition zone. All that remains is the ions in this zone which will create an internal electric field at the junction and which prevents the free charges remaining in each zone from crossing the junction to recombine. [17]

a) Migration of charges b) Electric field E moving towards the junction plane. Resulting, due to fixed charges.

Figure I.9: The pn junction.

I.7.3. Photovoltaic effect:

The conversion of solar energy into electrical energy is based on the photovoltaic effect, that is to say on the capacity of photons to create charge carriers (electrons and holes) in a material. When a semiconductor is illuminated with radiation of appropriate wavelength (the photon energy must be at least equal to that of the energy gap of the material), the absorbed photon energy allows electronic transitions from the band valence towards the conduction band of the semiconductor, thus generating electron-hole pairs, which can contribute to the transport of current (photoconductivity) by the material when it is polarized.

If we now illuminate a PN junction shown in Figure I.10, the electron-hole pairs which are created in the space charge region of the junction are immediately separated by the electric field which reigns in this region, and driven into the neutral zones on either side of the junction. If the device is isolated, a potential difference appears across the junction (photo voltage), if it is connected to an external electrical load, we observe the passage of a current even though no voltage is applied to the device. This is the basic principle of a photovoltaic cell. [18]

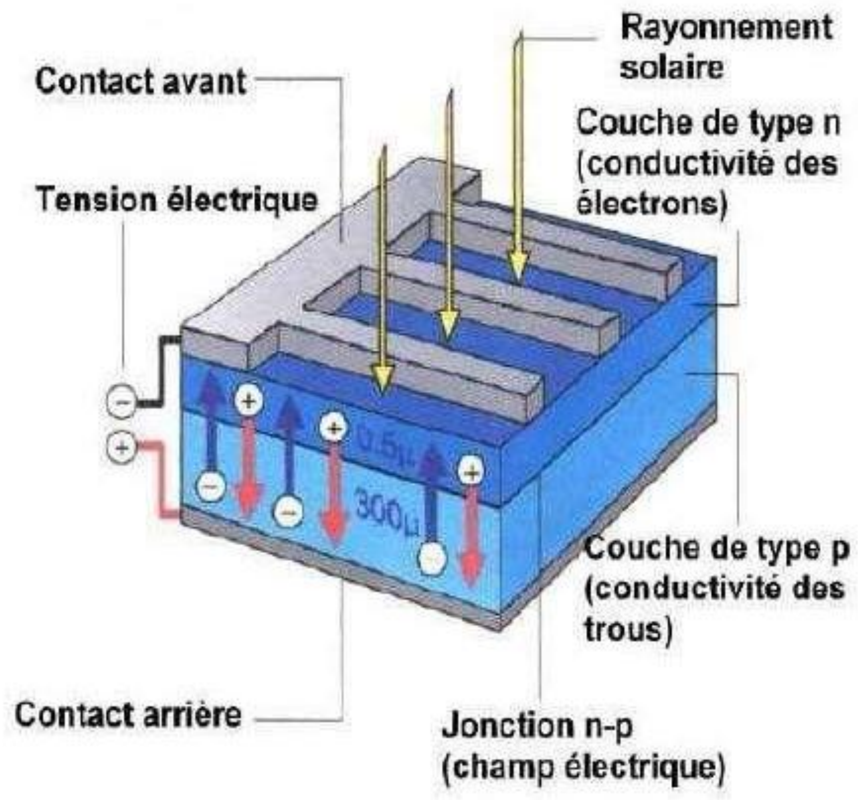

Figure I.10: The photovoltaic effect.

Principle of operation

To create an electric current in a semiconductor, it must be supplied with energy which allows electrons to be extracted from the valence band to transfer them to the conduction band, i.e. an energy greater than the forbidden band gap. Light whose photons carry energy: $E = h\upsilon$ makes it possible to achieve this effect: it is the photovoltaic effect.

Light penetrating into a semiconductor therefore allows, if its energy is greater than the gap, to cause the semiconductor to pass from the insulating state to the conducting state; this phenomenon increases when the temperature of the semiconductor rises. When an electron is removed from the valence band to pass into the conduction band, it leaves behind a vacancy or hole in its place, then another electron close to the valence band can fill that hole and leave behind in turn a hole, we will thus have established a current of holes. The two types of current will not be differentiated, we will simply speak of current, whether it is electrons or holes.

Similarly, it is said that the absorption of photon energy by the semiconductor creates pairs of electron-hole carriers. The photoelectric effect simply changes the electrical conductivity of certain semiconductors, this is used to make light-dependent resistors, components widely used in cameras and anywhere light needs to be measured. To transform the photosensitive semiconductor from a passive component into an active component, it is necessary to be able to generate a carrier current, therefore providing a force which will force the electrons and holes to flow in two opposite directions. This force will be produced by an internal electric field coming from the doping of the semiconductor.[19]

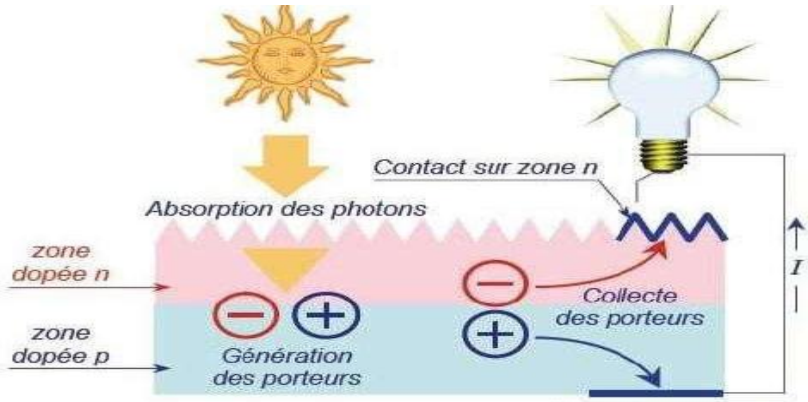

Figure I.11: The operating principle of a PV cell. [19]

I.7.4. Types of photovoltaic cells:

The different techniques used today have made it possible to develop various types of silicon cells: monocrystalline, poly-crystalline, amorphous.

There are also other types of cells that use other types of materials. has. Monocrystalline silicon cell

When cooling, the molten silicon solidifies, forming only one large crystal. We then cut the crystal into thin slices which will give rise to the cells.

These cells are generally a uniform blue. Monocrystalline cells are the most commercially available, offering good electrical efficiency of between 10% and 17%, but require a more complex and therefore expensive production method. Indeed, obtaining a pure crystal requires a large amount of energy. [28]

Figure I.12: Monocrystalline photovoltaic cell.

a) Poly-crystalline cell

As silicon cools in an ingot mold, several crystals form. The photovoltaic cell has a bluish appearance, but not uniform, we can see patterns created by the different crystals. Poly-crystalline cells have an electrical efficiency of between 11% and 15%. Their manufacturing process consumes less energy. They thus have a lower production cost but a slightly lower efficiency than that of monocrystalline cells [20].

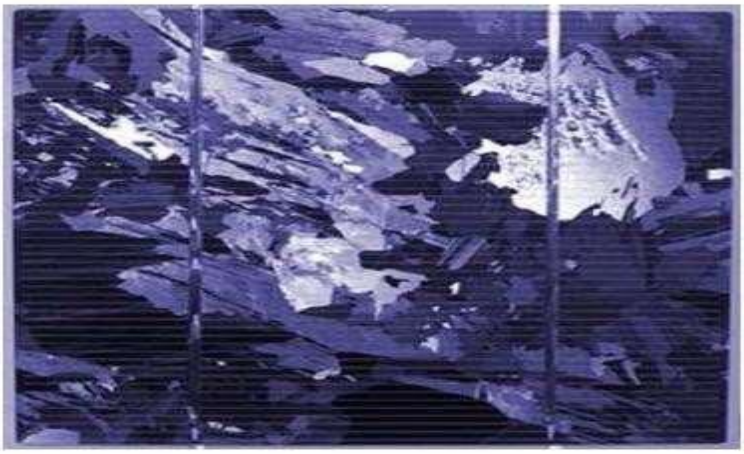

Figure I.13: Poly-crystalline photovoltaic cell.

b) Amorphous cell

Silicon during its transformation produces a gas, which is projected onto a sheet of glass. The cell is brown. This is the cell of calculators and so-called “solar” watches; their manufacturing costs are the most attractive, but they have an efficiency of between 5 and 7%. [20]

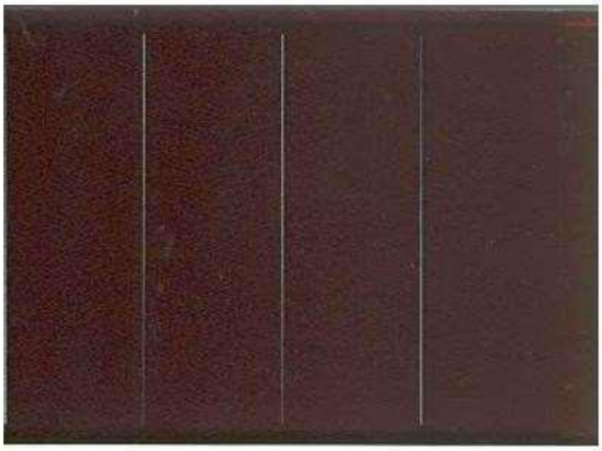

Figure I.14: Amorphous photovoltaic cell.

I.8. Conclusion

Meteorological data regarding radiation is essential for the design of a PV system. Because in the energy domain, the source defines the nature of the energy and the method of the exploit.

In this chapter, we have defined the main concepts which summarize the behavior of emitted solar radiation. Then, we carried out the modeling which links its different parameters.

Finally, we closed with a brief explanation of the principle of photovoltaic conversion in the structure of a solar cell.

Chapitre II

Modeling of photovoltaic system

II.1. Introduction

Solar cells or photovoltaic cells are components op to electronic which directly transform sunlight into electricity. They are made using semiconductor materials, that is to say having properties intermediate between conductors and insulators. The base material in most cases is silicon. Depending on the manufacturing process, we will obtain more photocells or less efficient, in amorphous form, polycrystalline, or mono crystalline [2].

Other materials can be used: Gallium Arsenide (AsGa), Cadmium Telluride (CdTe).

The operation of the photocell is based on the electronic properties acquired by silicon when small numbers of foreign atoms ("impurities") are substituted for silicon atoms in a crystal lattice: this is what we call the doping [21].

If the impurity atom contains more electrons than silicon, the material will contain excess free electrons: it will be called "N" type (e.g. phosphorus doping) [21].

If the impurity atom contains fewer electrons than silicon, the material will be electron deficient: it will be called "P" type (e.g. boron doping) [21].

A solar cell will be obtained by constituting a junction of two opposite type zones (PN junction) [16]. In the vicinity of the junction, an electric field appears caused by the imbalance of charges. It will help to drain the electrons which will have been detached by the energy of the incident photons (grains of light) [21].

Solar cells are generally combined in series and parallel, then encapsulated under glass to obtain a PV module

II.2. Equivalent circuit of a solar cell

Presentation and modulation of PV module:

The model does not take into account the internal losses of the current. A diode is connected in anti-parallel to the current generator light. The output current I is obtained by the Kirchhoff law:

$$I = I_{ph} - I_d \tag{II-1}$$

I_{ph}: is the photocurrent,

Id:is the diode current which is proportional to the saturation current and it is given by the equation

$$I_d = I_0[exp\left(\frac{V}{A*N_s*V_T}\right) - 1] \quad \text{(II-2)}$$

V: is the voltage imposed on the diode

$$V_T = K * T_c/q \quad \text{(II-3)}$$

I_0: is the reverse saturation or leakage current of the diode (A).

$V_{TC} = 26mV$at 300 K For silicon cell.

T_c: is the actual temperature of the cell (K).

K: Boltzmann constant $1.381*10^{-23}$ J / K

q: is the electron charge ($1.602*10^{-19}$ C).

V_T: is called thermal tension due to its exclusive temperature dependence[22].

Ns: is the number of PV cells connected in series.

A: is the Ideality Factor.

This depends on the photovoltaic cell technology and can be chosen from table 1. It should be emphasized that A is a constant which depends on the photovoltaic cell technology.

All terms by which, V is divided into equation (II.2)

Under the exponential function are inversely proportional to the cell

Table 1: Ideality factor (A) [18].	
Technology	ideality factor
Si-mono	1.2
Si-poly	1.3
a-Si-H	1.8
a-Si-H tandem	3.3
triple a-Si-H	5
cdTe	1.5
CTs	1.5
GaAs	1.3

The temperature and therefore, vary according to varying conditions. In this work, this term is designed by 'a' and called thermal voltage (V), the ideality factor, is considered constant and chosen in Table 1 according to the photovoltaic cell technology. The thermal tension "a" is presented by the equation (II.4)

$$a = \frac{N_s * A * K * T_c}{q} = N_s * A * V_T \quad \text{(II-4)}$$

In[19], 'a' is called "the modified ideality factor" and is considered a parameter to be determined, while A is the ideality of the diode (see table 2).

- **In the (Fig. 1b):**

In reality, it is impossible to neglect the series resistance Rs and the parallel resistance, due to their impact on the efficiency of the PV cell and the photovoltaic module. When is taken into consideration, the equation ($R_p R_s$II.2) should take the following form:

$$I_d = I_0[exp\left(\frac{V+I*R_s}{q}\right) - 1] \quad \text{(II-5)}$$

Of course, fig. 1b is a simplified form, easy to implement in simulators. But Fig. 1c is the most representative of the cell.PV

- **In the (Fig. 1c)**

By applying Kirchhoff's law, the current will be obtained by the equation:

$$I = I_{ph} - I_d - I_p \quad \text{(II-6)}$$

I_p: is the current leakage in parallel resistance.

According to the equation (II.7), the output current of a module containing N cells in series will be:

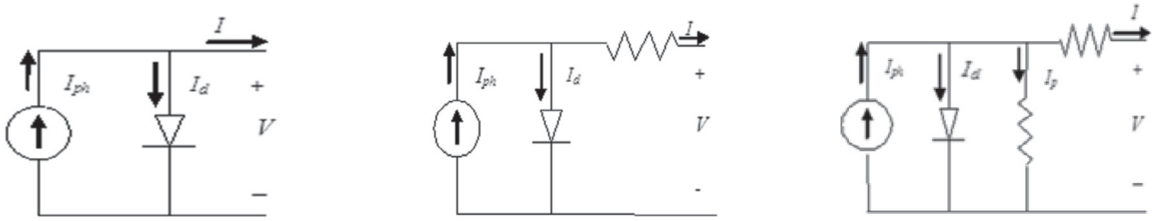

a) Ideal single diode model b) Practical model with Rs c) Practical model with Rs and Rp

Figure II.1: The equivalent circuit of a solar cell and a photovoltaic device.

Table 2 PWX 500 PV module (49 W) characteristics	
Settings	Value
Pmp (W)	49
Imp (A)	2.88
Vmp (V)	17
Isc (A)	3.11
Voc (V)	21.8
RS (O)	0.55
Noct °C	45
lsc (K°)	1.3 Æ $10^{—3}$
Kd (K°)	—72.5 Æ $10^{—3}$
N_s	36

$$I = I_{ph} - I_0 \left[exp\left(\frac{V+I*R_s}{q}\right) - 1\right] - \frac{V+R_s*I}{R_p} \quad \text{(II-7)}$$

It is not easy to determine the parameters of this transcendental equation. But this model offers the best match with experimental values.

II.3. Determination of parameters:

The number of parameters varies depending on the Model choices and the hypotheses adopted by the researchers. For Example, In[20], [21],It is considered that I_{ph}, I_0, R_s ,R_p and the ideal factor are five parameters which depend on the incident solar radiation and the temperature of the cell. While [22], [23] the unknown parameters are: I_{ph}, I_0 ,R_s and γ as well as:

$$\gamma = N_s * A$$

In this work, the four parameters to be evaluated are also I_{ph}, I_0, R_s, R_p

II.3.1. Determination of I_{ph}:

According to Fig. 1 a, the output current at standard test conditions (STC) is:

$$I = I_{ph,ref} - I_{0,ref}[exp\left(\frac{V}{a_{ref}}\right) - 1] \quad \text{(II-8)}$$

This equation makes it possible to quantify $I_{ph,\ ref}$ which cannot be determined otherwise. When the PV cell is short circuited:

$$I_{sc,ref} = I_{ph,ref} - I_{0,ref}\left[exp\left(\frac{0}{a_{ref}}\right) - 1\right] = I_{ph,ref} \quad \text{(II-9)}$$

But this equation is only valid in an ideal case. So the equality is not correct. Then, equation (II.10) should be written as follows:

$$I_{ph,ref} = I_{sc,ref} \quad \text{(II-10)}$$

The photocurrent depends on both irradiance and temperature

$$I_{ph} = \frac{G}{G_{ref}}(I_{ph,ref} + \mu_{sc} * \Delta T) \quad \text{(II-11)}$$

G: Irradiation (W/m^2)

G_{ref}: Irradiation at STC = 1000 W/m^2

ΔT= $-T_c - T_{c,ref}$ (Kelvin)

$T_{c,ref}$: Cell temperature at STC = 25+ 273 = 298 K

I_{sc}: Short-circuit current temperature coefficient (A/K) provided by the manufacturer,

$I_{ph,ref}$: Photocurrent (A) at STC.

II.3.2. Determination I_0:

The R_P shunt resistance is generally considered excellent, so the last term of the relation (II 8) should be eliminated for the next approximation. by applying equation (II.8) to the three most notable points in the standard test state: the open circuit voltage (I=0, V = $V_{oc,ref}$) the short circuit current (V=0, I = $I_{sc,ref}$) and the voltage ($V_{mp,ref}$) and current ($I_{mp,ref}$) At maximum power, the following equations can be written:

$$I_{sc,ref} = I_{ph,ref} - I_{0,ref}[exp\left(\frac{I_{sc,ref}*R_S}{a_{ref}}\right) - 1] \quad \text{(II-12)}$$

$$0 = I_{ph,ref} - I_{0,ref}[exp\left(\frac{V_0}{a_{ref}}\right) - 1] \quad \text{(II-13)}$$

$$I_{sc,ref} = I_{ph,ref} - I_{0,ref}[exp\left(\frac{V_{pm,ref}+I_{pm,ref}*R_S}{a_{ref}}\right) - 1] \quad \text{(II-14)}$$

The term (-1) must be neglected because it is much smaller than the exponential term. According to equation (11), and by replacing ($I_{ph,\ ref}$) with equation (II.14):

$$0 = I_{sc,ref} - I_{0,ref}\ exp\left(\frac{V_{oc,ref}}{a_{ref}}\right) \quad \text{(II-15)}$$

$$I_{0,ref} = I_{sc,ref}\ exp\left(\frac{-V_{oc,ref}}{a}\right) \quad \text{(II-16)}$$

$$I_0 = DT_c^3 exp\left(\frac{-q*\varepsilon_G}{A*K}\right) - 1 \quad \text{(II-17)}$$

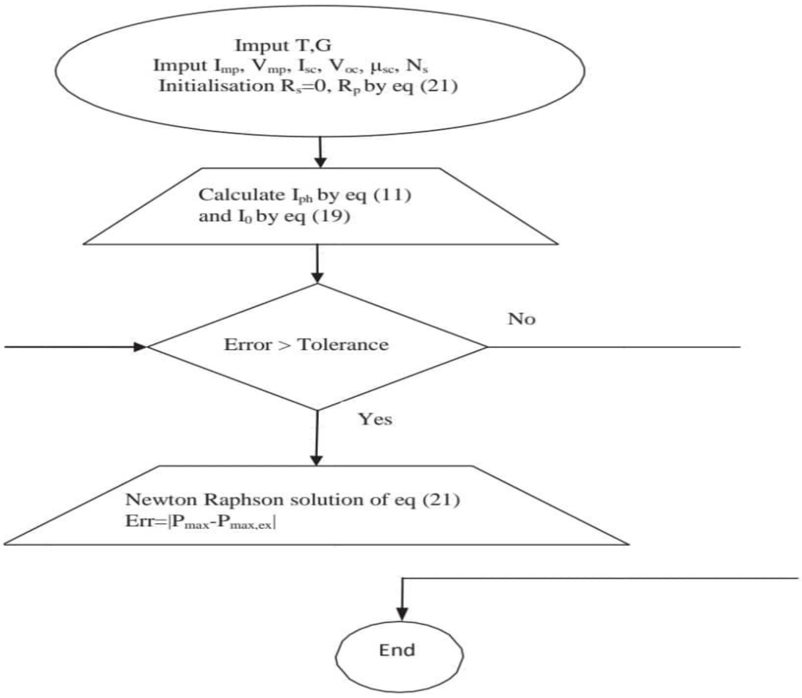

Figure II.2: Iteration flow chart.

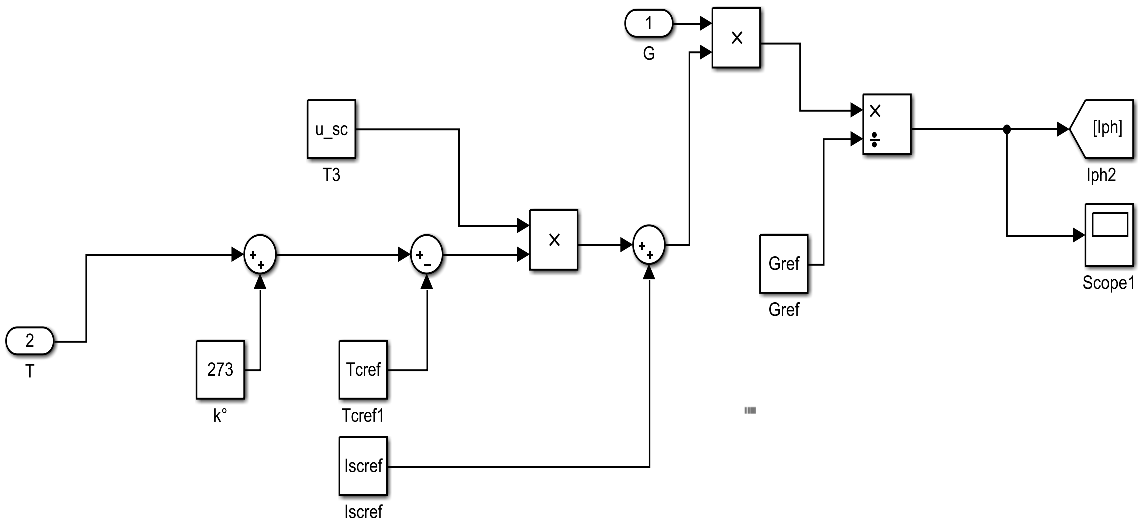

Figure II.3: Detailed deployment.I_{ph}

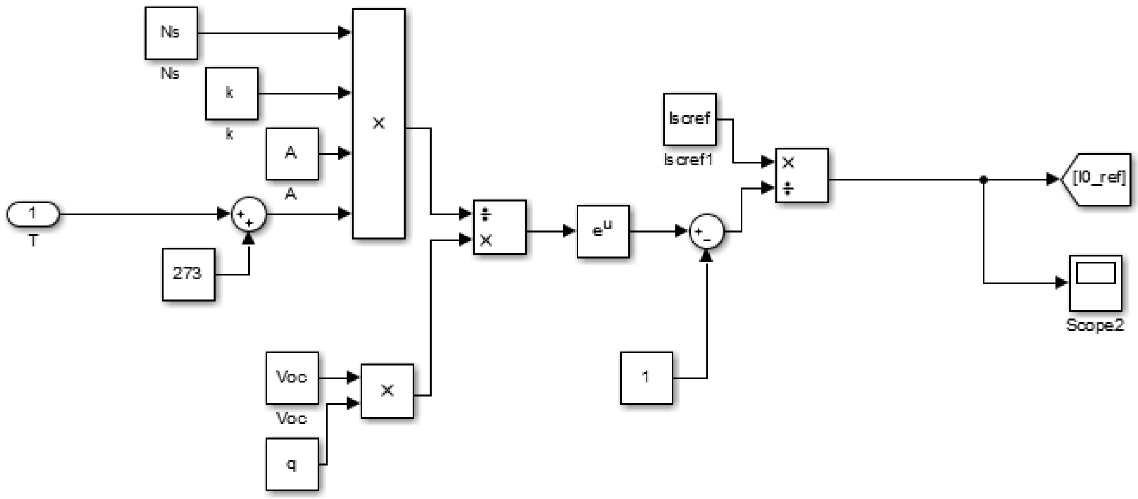

Figure II.4: Detailed deployment.$I_{0,ref}$

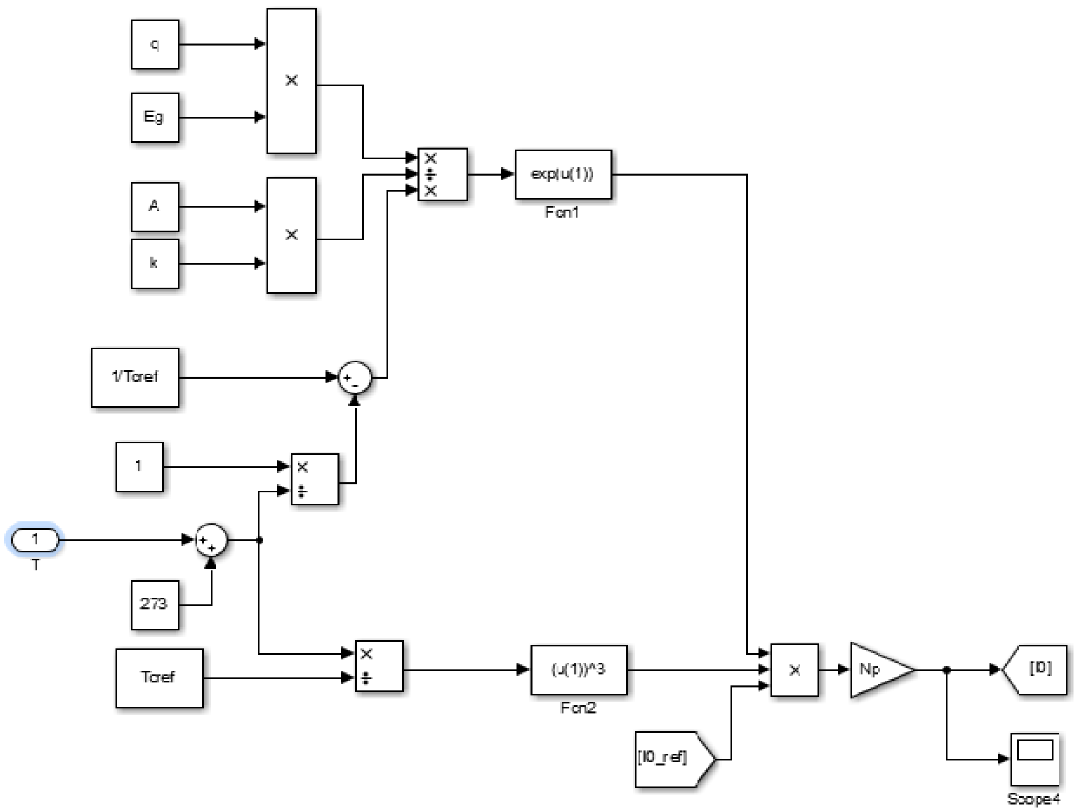

Figure II.5: Detailed deployment.I_0

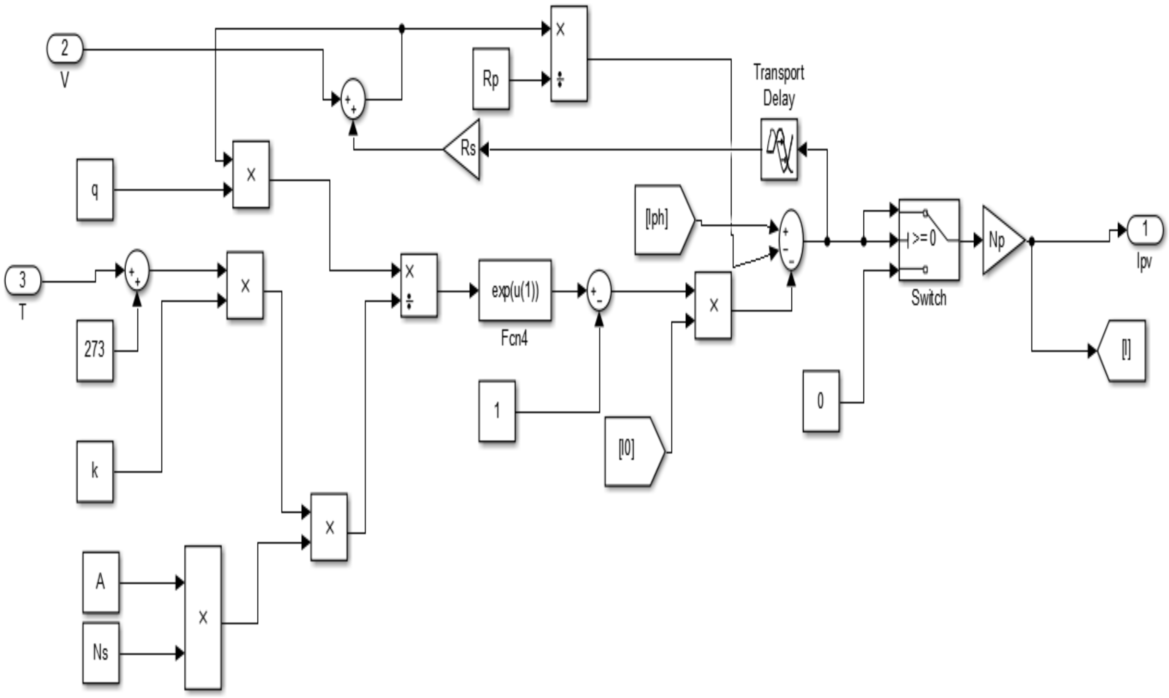

Figure II.6: Detailed deployment.I_{pv}

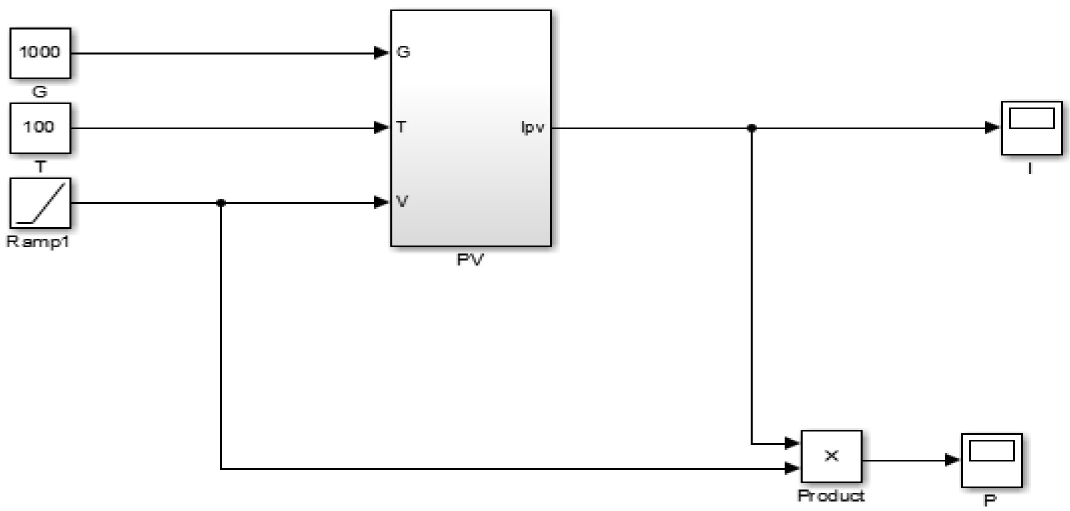

Figure II.7: presentation of PV module

II.4. Constitution of a photovoltaic generator (GPV):

The combination of several photovoltaic cells in series/parallel gives rise to a photovoltaic generator. If cells connect in series, the voltages of each cell add together, increasing the total generator voltage. On the other hand, if the cells are connected in parallel, the amperage will increase as shown in the following figures.

II.4.1. Association of parallel photovoltaic cells:

The properties of parallel grouping of cells are dual to those of series grouping. Thus, in a group of cells connected in parallel, the cells are subjected to the same voltage and the resulting characteristic of the group is obtained by adding the currents at a given voltage. Figures (II. (9; 10)) show the resulting characteristics (I_{PCC}, V_{PCO}) obtained by associating in parallel (index p) Np identical cells:

$$I_{pcc} = N_p * I_{cc} \qquad and \qquad V_{pco} = V_{co}$$

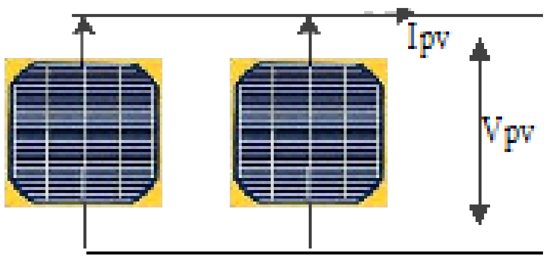

Figure II.8: Diagram of 2 photovoltaic cells associated in parallel

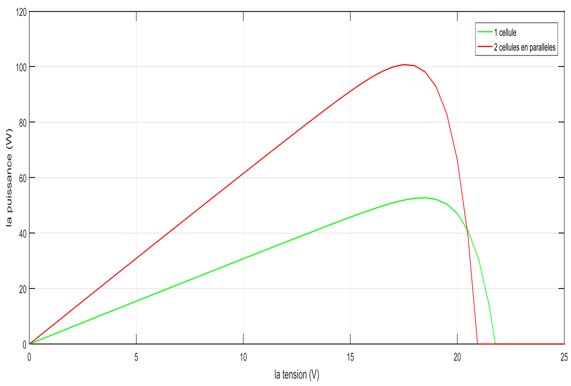

Figure II.9: PV characteristic of PV cells connected in parallel.

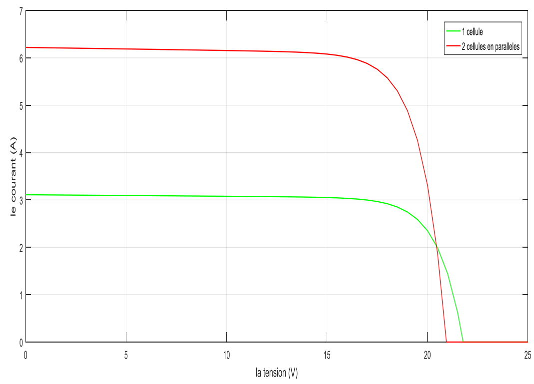

Figure II.10: Characteristic IV of PV cells connected in parallel

II.4.2. Association of photovoltaic cells in series:

In a series arrangement, the cells carry the same current and the resulting characteristic of the series arrangement is obtained by adding the voltages at a given current. The figures (II. (12; 13)) show the resulting characteristic (I_{SCC}, V_{SCO}) obtained by associating in series (index s) Ns identical cells (I_{CC}, V_{CO}):

$$I_{scc} = I_{cc} \quad \text{and} \quad V_{sco} = N_s * V_{co}$$

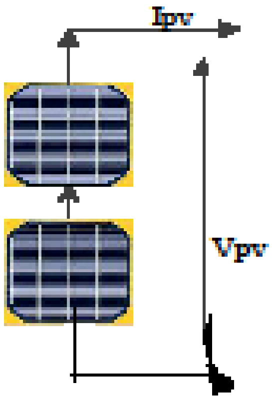

Figure II.11: 3 cell diagram photovoltaics associated in series

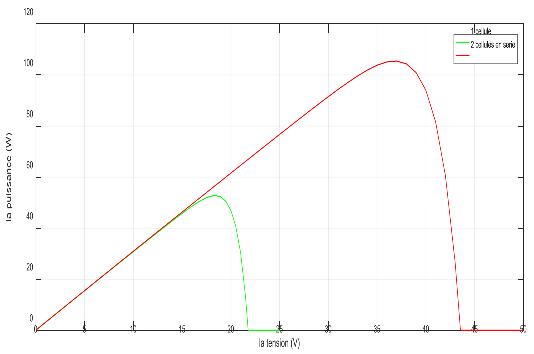

Figure II.12: PV characteristic of cell photovoltaic cells connected in series

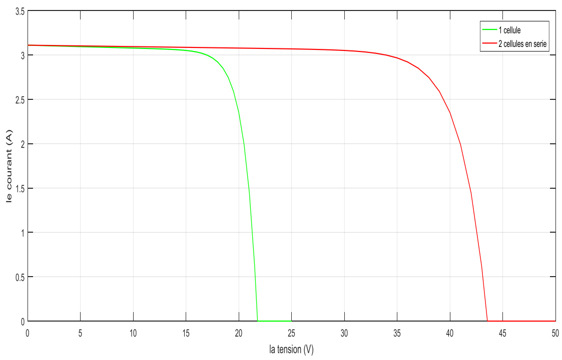

Figure II.13: IV characteristic of cells photovoltaic connected in serie

Most commercial photovoltaic panels are made up of sub-arrays of cells connected in series. Each of these subnetworks is itself made up of a group of photovoltaic cells connected in series. The number of cells per subnetwork is the result of an economic compromise between protection and losses of a significant part of the photovoltaic generator in the event of a partial fault.

The demonstration site, CDER, is currently equipped with 3 panels, (figure A.1, in the appendix), each of them is made up of several modules connected together in series and in parallel, referenced: ISOFOTON 106 W MONOCRISTALLINE, ridges and structured as shown in figure (II -14) Ipv

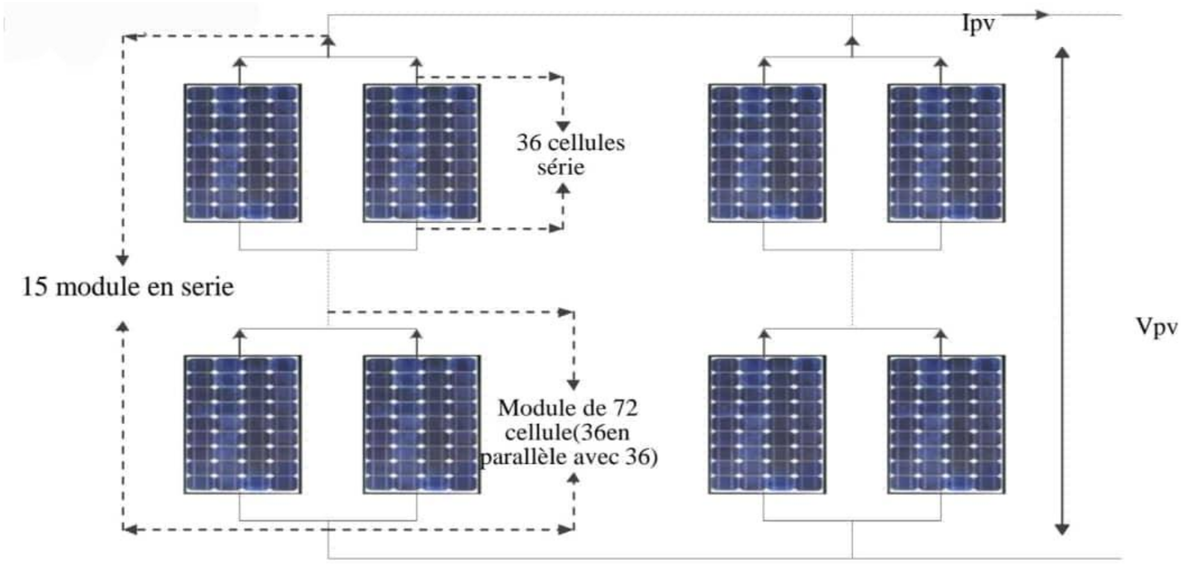

Figure II.14: Diagram of part of the electricity production plant of photovoltaic system installed at CDER.

The maximum power delivered by the photovoltaic panel given by the product between the voltage Vop and the current Iop as represented by the following formula:

$$P_{max} = V_{op} * I_{op}$$

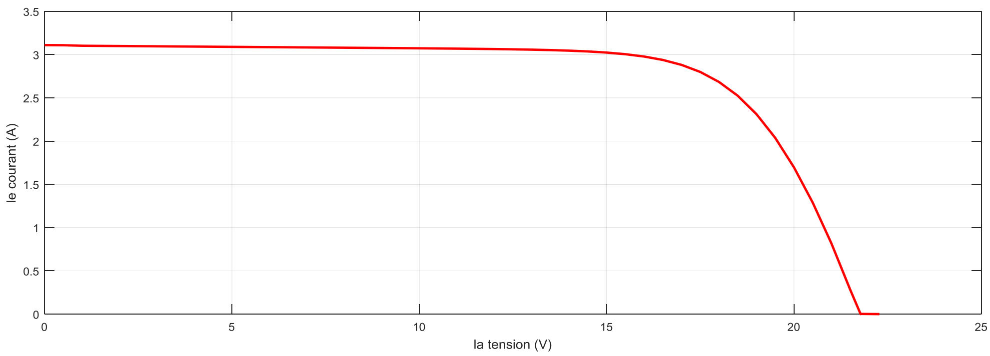

Figure II.15: Characteristic IV of a photovoltaic generator

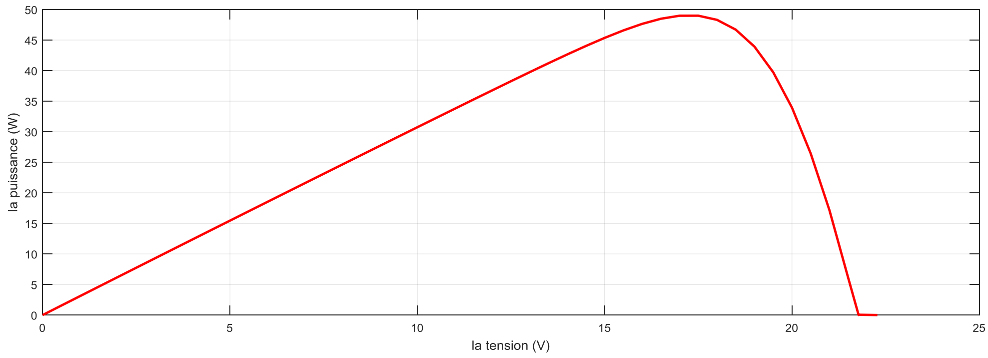

Figure II.16: PV characteristic of a photovoltaic generator.

II.5. Influence of Illumination:

By varying the illuminance between 200 w/m² and 1000 w/m², the characteristic (*Ipv=f(Vpv)*) is given by figures (II. (17,18)). Note that the value of the short-circuit current is directly proportional to the intensity of the radiation. On the other hand, the open circuit voltage does not vary in the same proportions, it remains almost identical even at low illumination.

The standard irradiation internationally accepted for musere the response of photovoltaic panels is a radiant intensity of 1000W/m^2 and a temperature $25.m^2C^0$

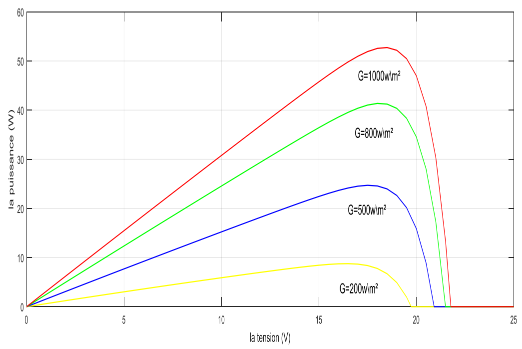

Figure II.17: PV characteristic of the Module PV depending on lighting.

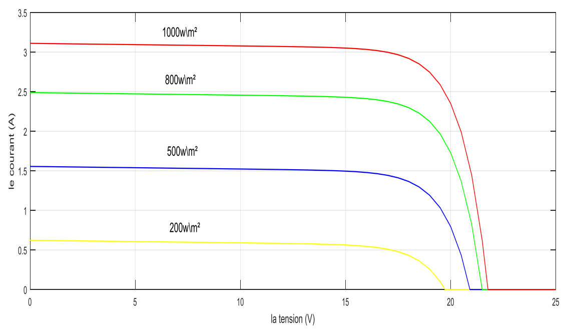

Figure II.18: Characteristic IV of the PV module according to illuminance

II.6. Influence of Température:

By varying the temperature from 0°C to 75°C, the characteristic ($I_{pv}=f(V_{pv})$) is given by figures (II.(19,20)). We note that the temperature has a negligible influence on the value of the short-circuit current. On the other hand, the open circuit voltage drops quite sharply when the temperature increases, consequently the extractable power decreases. When sizing an installation, the variation in site temperature must be taken into account.

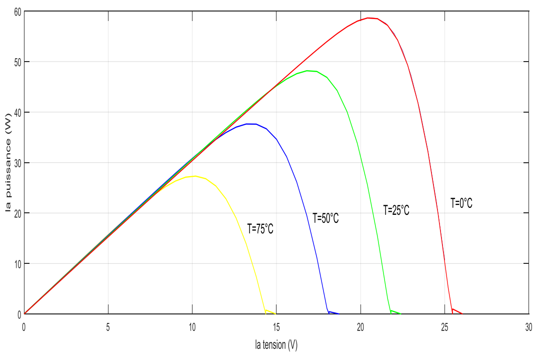

Figure II.19: PV characteristic of the module PV according to température

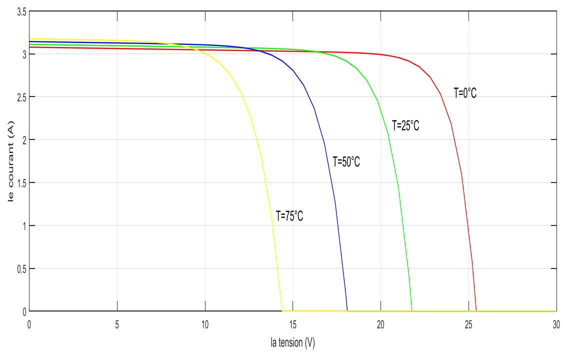

Figure II.20: Characteristic IV of the PV module according to temperature

II.7. Influence of series resistance:

Figure (II (21-22) shows the influence of the series resistance on the IV characteristic of the cell which results in a decrease in the slope of the PV power curve in the area where the cell functions as a voltage generator constant.

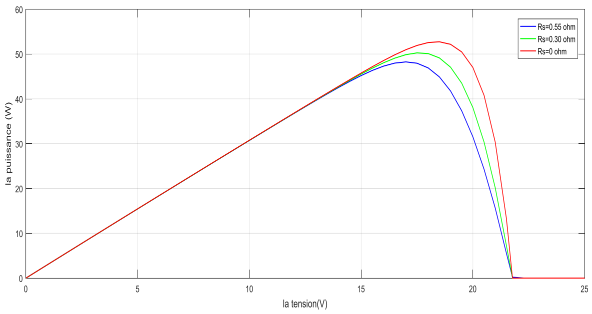

Figure II.21: PV module characteristic PV according to series resistance

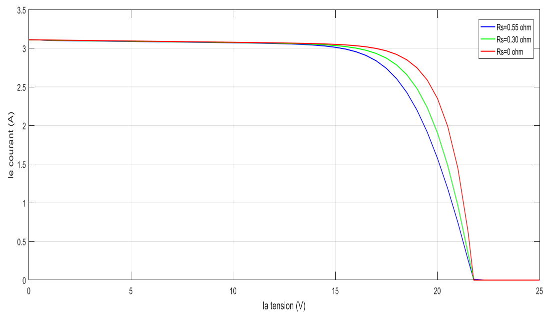

Figure II.22: Module Characteristic IV PV according to series resistance

II.8. Influence of Illuminatio and temperature:

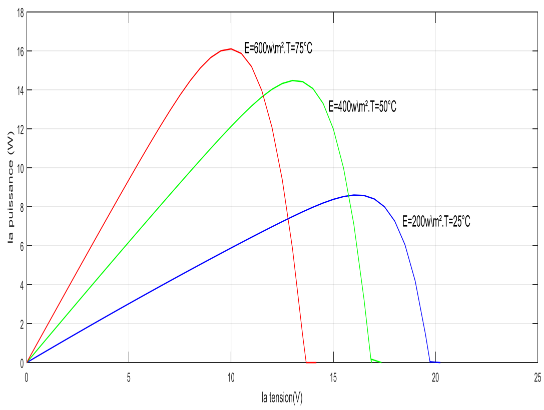

Figure II.23: PV module characteristic according to illuminance and PV temperature

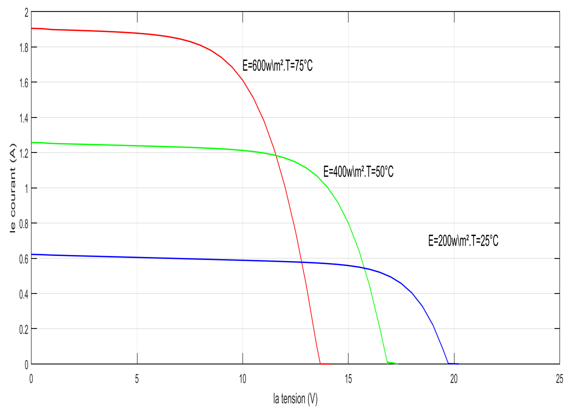

Figure II.24: Module Characteristic IVPV according to Illuminance and temperature

II.9. Influence of ideality factor:

Theoretically, the idiolity factor A of poly-crystalline cells takes a value between 1 and 2, while being close to the value of 1 compared to high currents, it increases to the value for low currents. for normal operation it is generally equal to 1.3. the curve of the figure (II -25) confirms the previous notification.

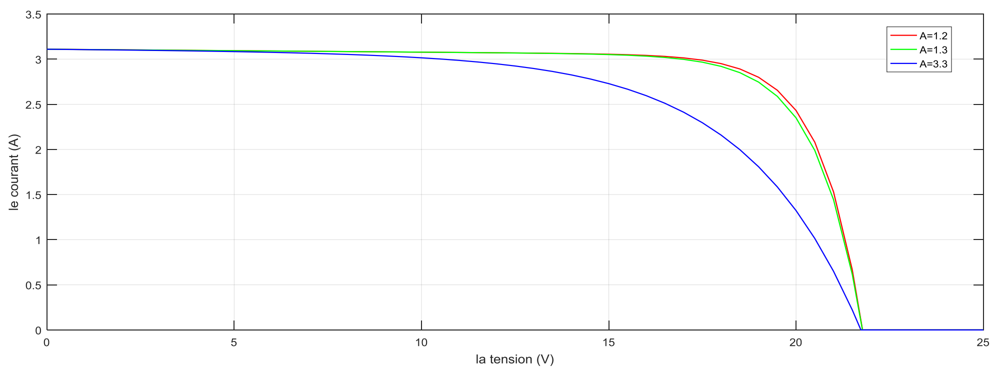

Figure II.25: Characteristic IV of PV module according to Illuminance and temperature

II.10. DC-DC converters (chopper):

Chopper are DC-DC type converters making it possible to control electrical power in circuits operating in direct current with great flexibility and high efficiency [23].

The chopper consists of capacitors, inductor and switches. In the ideal case, all these devices do not consume any active power, this is the reason why we have good efficiencies in the choppers [23].

The cutting technique, which appeared around the 1960s, provided a solution to the problem of poor efficiency and bulkiness of series power supplies.

In a switching power supply (Figure II.26), the input voltage is "chopped" at a given frequency by a transistor alternately on and off.

This results in a voltage square wave that simply needs to be smoothed to finally obtain a DC voltage [23].

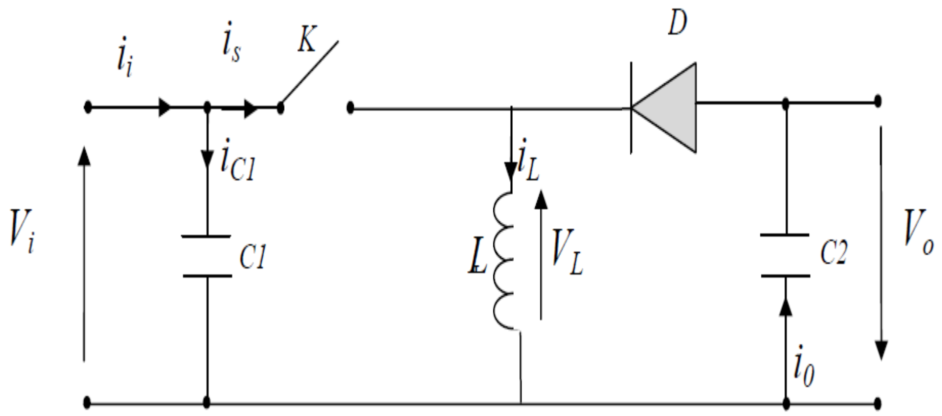

Figure II.26: Schematic diagram of a type of switching power supply

From a circuit point of view, the chopper appears as a quadrupole (Figure II.27), playing the role of a connecting element between two parts of a network. It can be considered as a transformer of continuous electrical quantities [23].

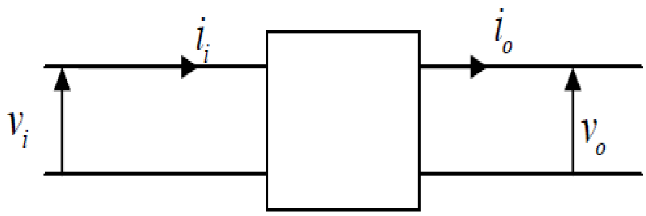

Figure II.27: Diagram of an electric quadrupole

Regulation of the output voltage at a constant level is achieved by an action on the "duty cycle", defined as the fraction of the switching period where the switch is conducting (Figure II.28). The switch is an on-off (off-saturated) semiconductor device, usually a MOSFET transistor. If the semiconductor device is blocked, its current is zero and therefore its power dissipation is zero. If the device is in the saturated state the voltage drop across its terminals will be almost zero and therefore the power lost will be very small [23].

During operation of the chopper, the transistor will be switched at a constant frequency f with a closing time = Tds and an opening time = (1-d) Ts. Or:

- T_S: is the switching period which is equal to $1/f_s$
- d: the duty cycle of the switch (d ∈ [0, 1]).

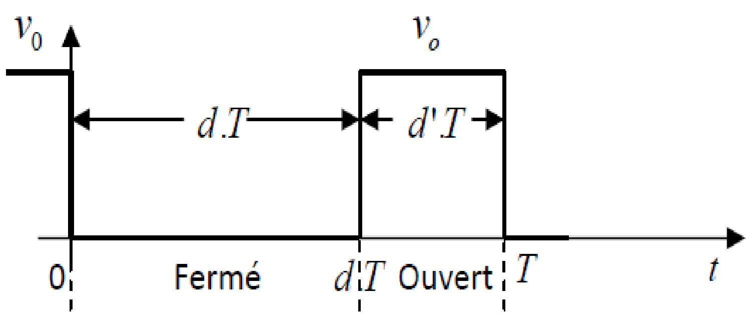

Figure II.28: closing and opening periods of a switch.

There are several types of DC-DC converters. Among which, we present the principle of the three types of switching converters (buckle, booster and mixed), frequently used in photovoltaic systems to generate the desired voltages and currents as well as for the adaptation of solar panels with the different loads [25 26 27 28].

II.10.1. Step-down chopper:

The buck converter can often be found in the literature under the name of buck chopper or series chopper. (Figure II.29). presents the principle diagram of the buck converter. Its typical application is to convert its input voltage into a lower output voltage, where the conversion ratio M=V_0/V_i - changes with the ratio cyclic of the switch.

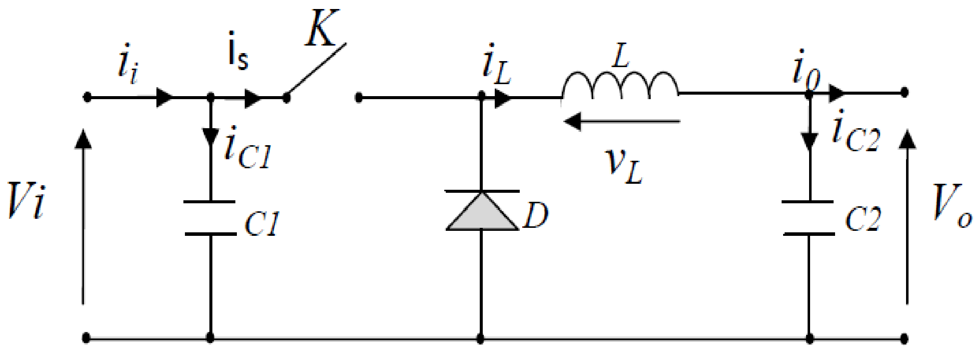

Figure II.29: Schematic diagram of a buck converter.

Knowing the real behavior of this converter requires knowing its mathematical model in detail.

For this we must represent the equivalent circuit by the two states of the switch and subsequently draw the mathematical model linking the input/output variables. (Figure II.30) shows the diagrams of the equivalent circuits of a buck converter in the two cases: the switch closed during dTs and the switch open during (1-d) T_s [25 26 29 30].

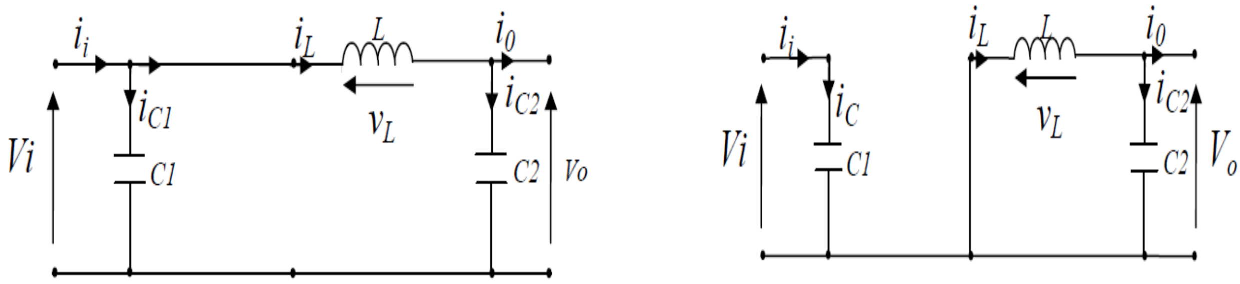

(a) **Figure II.30:** Equivalent diagrams of the step-down chopper, (a) K closed, (b): open

By applying Kirchhoff's laws to the two circuits in figure (II.32), we obtain the following systems of equations:

For the first period d.Ts:

$$I_{c_1}(t) = C_1 \frac{dV_i}{dt} i_i(t) - i_L(t)$$

$$I_{c_2}(t) = C_2 \frac{dV_0}{dt} i_L(t) - i_0(t) \qquad \text{(II-18)}$$

$$V_l(t) = L \frac{dL_i}{dt} V_i(t) - V_0(t)$$

For the second period (1-d)T_s:

$$I_{c_1}(t) = C_1 \frac{dV_1(t)}{dt} = i_i(t)$$

$$I_{c_2}(t) = L \frac{di_L}{dt} = i_L(t) - i_0(t) \qquad \text{(II-19)}$$

$$V_l(t) = C_1 \frac{dL_i}{dt} = -V_0(t)$$

To find a dynamic representation valid for the entire period Ts, we generally use the following expression [23]:

$$\left(\frac{dx}{dt}\right) T_s = \frac{dx}{dt_{DT_S}}\ dT_s + \frac{dx}{dt_{(1-D)T_S}}\ (1-d)T_s \qquad \text{(II-20)}$$

By applying the relation (II.20) to the systems of equations (II.18) and (II.19), we obtain the equations which govern the system over an entire period:

$$C_1 \frac{dV_i(t)}{dt} T_s = dT_s(i_i - i_L) + (1-d)T_s i_i$$

$$C_2 \frac{dV_0(t)}{dt} T_s = dT_s(i_L - i_0) + (1-d)T_s(i_L - i_0) \qquad \text{(II-21)}$$

$$L \frac{dL_i}{dt} = dT_s(V_i - V_0) + (1-d)T_s(-V_0)$$

After arrangement, we obtain:

$$i_0(t) = i_l(t) - C_2 \frac{dV_0(t)}{dt}$$

$$i_L(t) = \frac{1}{d}\left(i(t) - C_1 \frac{dV_i(t)}{dt}\right) \qquad \text{(II-22)}$$

$$V_i(t) = \frac{1}{d}\left(L\frac{di_L(t)}{dt} + V_0(t)\right)$$

II.10.2. Booster chopper:

The latter is a boost converter, also known as a “boost” or parallel chopper; its basic schematic diagram is that of (Figure II.31). Its typical application is to convert its input voltage to a higher output voltage [23].

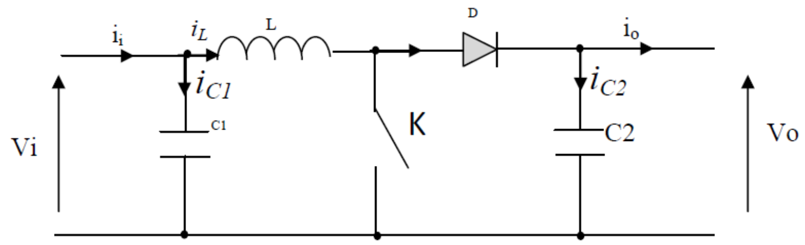

Figure II.31: Schematic diagram of a Boost converter

As for the buck converter, the application of Kirchhoff's laws on the equivalent circuits of the boost converter (see Figure II.32) of the two operating phases gives [23].

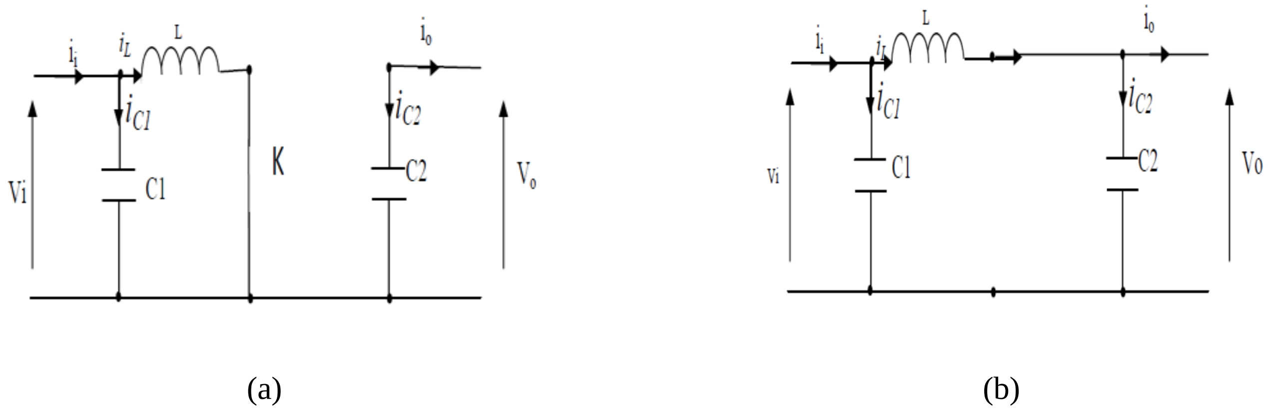

Figure II.32: Equivalent diagrams of the booster chopper

(a): K closed, (b): open

II.10.3. Buck-boost chopper:

The buck-boost converter combines the properties of the previous two converters, it is used as an ideal transformer from any input voltage to any desired output voltage; its basic diagram is illustrated by (Figure II.33) [23].

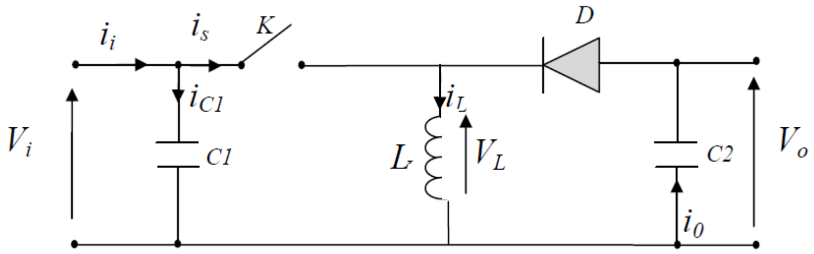

Figure II.33: Buck-boost converter

(Figure II.34) shows the two equivalent diagrams of the buck-boost converter for the two two-cycle operations [23].

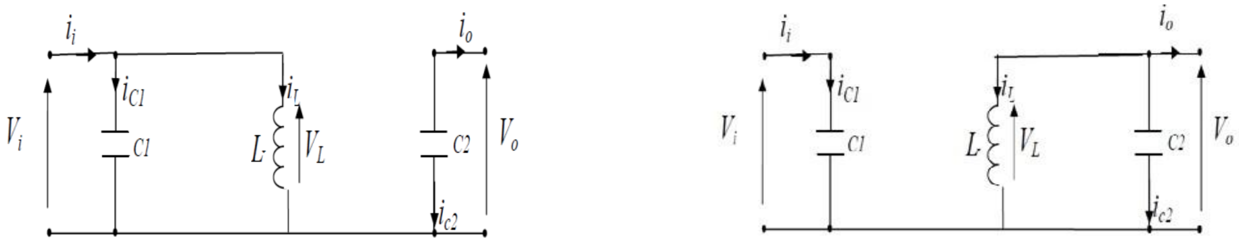

(a) (b)

Figure II.34: Equivalent diagrams of the buck-boost chopper,

(a): K closed, (b): K open

For the first period d.Ts:

$$I_{c_1}(t) = C_1 \frac{dV_i(t)}{dt} = i_i(t) - i_L(t)$$

$$I_{c_2}(t) = C_2 \frac{dV_0(t)}{dt} = -i_0(t) \quad \text{(II-23)}$$

$$V_l(t) = L\frac{dL_i}{dt} = V_i(t)$$

For the second period (1-d)Ts

$$I_{c_1}(t) = C_1 \frac{dV_i(t)}{dt} = i_i(t)$$

$$I_{c_2}(t) = C_2 \frac{dV_0(t)}{dt} = i_L(t) - i_0(t) \qquad \text{(II-24)}$$

$$V_l(t) = L \frac{dL_i}{dt} = V_0(t)$$

we find the approximate model of the boost converter [23].

$$i_L = \frac{1}{d}(i_i - C_1 \frac{dV_i(t)}{dt})$$

$$i_0 = (1-d)i_L - C_2 \frac{dV_0(t)}{dt} \qquad \text{(II-25)}$$

$$V_l = \frac{1}{d}(-(1-d)V_0 + L \frac{di_L}{dt})$$

II.11. conclusion:

This chapter is dedicated to presenting the different components of a photovoltaic system.

We studied the principle of the photovoltaic effect, the PV cell and its parameters. Then we do a reminder of PV systems and their performances and it studies the adaptation stage between a PV generator and a load which presents the DC-DC converter (chopper).

In the next chapter, we present the MPPT command to find the point where the power of the photovoltaic generator is maximum.

Chapitre III

Pursuit of the maximum power point

III.1. Introduction:

We saw in the previous chapter that the characteristics of a photovoltaic generator depend on solar irradiance and temperature. These climatic variations lead to fluctuations in the maximum power point.

In order to extract, at any time, the maximum power available at the terminals of the GPV and transfer it to the load, an adaptation stage is used. This stage plays the role of interface between the load and the GPV. It ensures, through a control action, the transfer of the maximum power supplied by the generator.

The adapter commonly used in PV is a static converter (DC/DC power converter). The conversion structure is chosen according to the load to be supplied.

In this chapter we will study the direct connection between the photovoltaic generator and the load. The DC-DC converter used in our photovoltaic system is of the Boost type. Thus, we describe the MPPT control of DC-DC converters by the disturbance and observation (P&O) algorithm and the P&O algorithm improved by fuzzy logic in addition to an MPPT algorithm based entirely on fuzzy logic.

III.2. Direct connection between photovoltaic generator and load:

The simplest system that can be designed consists of a GPV photovoltaic generator and a load that directly uses the energy produced from the GPV. This energy is strongly dependent on illumination, temperature and the nature of the load.

Direct connection is mainly used because of its simplicity of implementation, its low cost due fundamentally to the absence of electronics [9]. But, it does not guarantee optimal transfer of energy from the GPV to the load. This configuration is illustrated in figure (III.1).

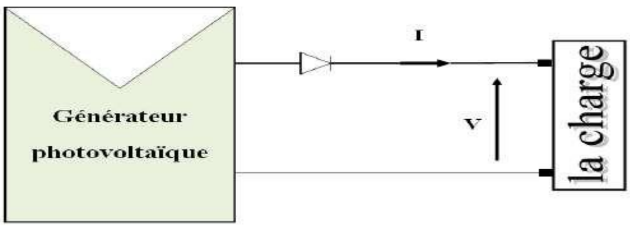

Figure III.1: Direct GPV-load coupling

III.3. Power converter:

The power adaptation stage is carried out by means of a static power converter which are devices which transform the available electrical energy into a form suitable for powering a load. [24]

The voltage supplied by the photovoltaic panels is a direct type voltage to adapt it to our needs there are some DC-DC converters (the choppers).

III.3.1. DC/DC converter

Figure III.2 shows the representation of a DC/DC converter [25].

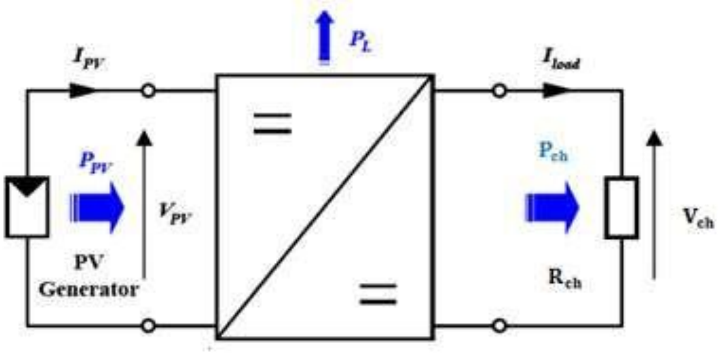

Figure III.2:DC/DC converter

The role of the DC/DC converter (in the context of PV) is to make the adaptation between the source (GPV) and the load for maximum power transfer. This is done by maintaining the operating point at or close enough to the MPP for any operating conditions (radiation, temperature, load characteristic, etc.).

In the following, the operating principle of a DC/DC converter of type Boost is described.

III.3.2. Boost converter:

A Boost converter, or parallel chopper, is a switching power supply which converts a DC voltage into another DC voltage of higher value. This type of converter is used as a source-load adapter, to extract the maximum power from GPV.

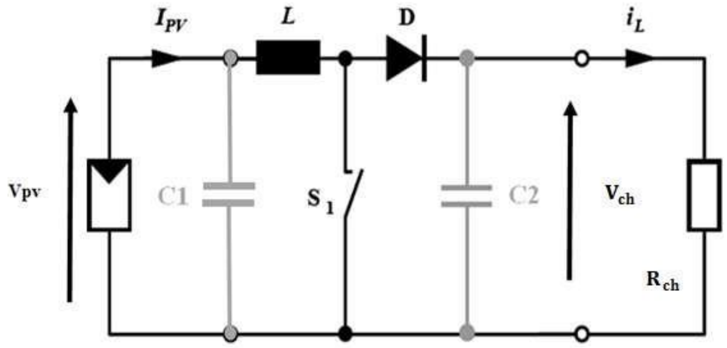

Figure III.3: Electrical diagram of a Boost converter

When switch S_1 is activated, the load voltage immediately drops to zero if capacitor C1 is discharged. The current IL flows through the inductance L following equation [26]:

$$\frac{di_L}{dt} = \frac{V_{pv}}{L} \qquad \text{(III-1)}$$

When S_1 is deactivated, the inductance is in series with the generator and its f.e.m is added to that of the generator (boost effect). The current i_L passing through the inductor then passes through the diode D, the capacitor C1 and the load. This results in a transfer of the energy accumulated in the inductor to the capacitor. The current then gradually decreases, because $V_{ch} > V_{PV}$:

$$\frac{di_L}{dt} = \frac{V_{pv} - V_{ch}}{L} \qquad \text{(III-2)}$$

Diode D prevents capacitor C1 from discharging when the switch is activated. The capacitor is assumed to be large enough to be able to smooth the voltage of the load.

The load voltage is given by:

$$V_{ch} = \frac{T}{t_{off}} V_{pv} = \frac{1}{1-D} V_{pv} \qquad \text{(III-3)}$$

With $D = \frac{t_{on}}{T}$: is the duty cycle (0< D < 1).

In our work, we consider the behavior of the circuit in continuous conduction, in this case cited above, the adaptation between the source and the load is carried out by choosing adequate values of the duty cycle.

III.4. Pursuit of maximum power point:

Improving the efficiency of the PV system requires maximizing the power of the PV generator. This is possible if the operating point is chosen well by adapting the impedance of the load to the source. The DC-DC converter will play the role of an impedance adapter thus ensuring operation at the optimal point which allows the maximum power of the PV generator to be produced [27].

Therefore, maximizing the power of a photovoltaic source amounts to seeking this optimal operating point. This control is called maximum power point follower. These MPPT methods are based on iterative search algorithms to find the operating point of the solar module so that the power generated is maximum without interruption of system operation. They are based on the permanent maximization of the power generated by photovoltaic PV modules.

The extracted power is calculated from the current and voltage measurements of the module and the multiplication of these two quantities. These measurements are used by various algorithms that pursue the actual MPP. There are several types of MPPT algorithms, among which we present the principle of the disturbance and observation algorithm and the MPPT algorithm based on fuzzy logic.

III.4.1. Perturbation and observation algorithm (P&O):

The perturb and observe algorithm is considered the most commonly used MPPT algorithm among other techniques due to its simple structure and ease of implementation. It is based on the concept that on change the PV generator power equals zero ($\Delta P_{pv} = 0$) at the top of the PV curve, as shown in (Figure III.4). P&O works by periodically perturbing (incrementing or decrementing) the PV generator voltage and comparing the corresponding generator output power P(k) to that of the previous disturbance P(k-1). If the terminal voltage disturbance results in an increase in PV power ($\Delta P_{pv} > 0$), the disturbance must be kept in the same direction, otherwise the disturbance is moved in the opposite direction. The disturbance cycle is repeated until reaching the maximum power at ($\Delta P_{pv} = 0$). The P&O organization chart is shown in (Figure III.5) [28].

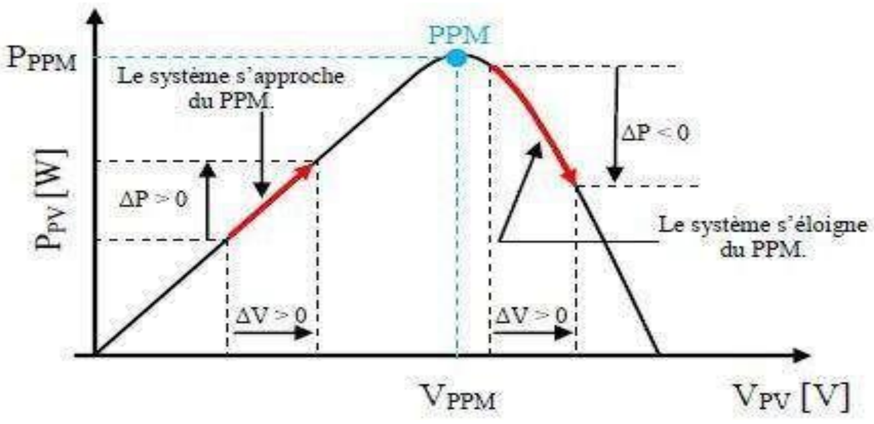

Figure III.4: Search for PPM by the (P&O) method

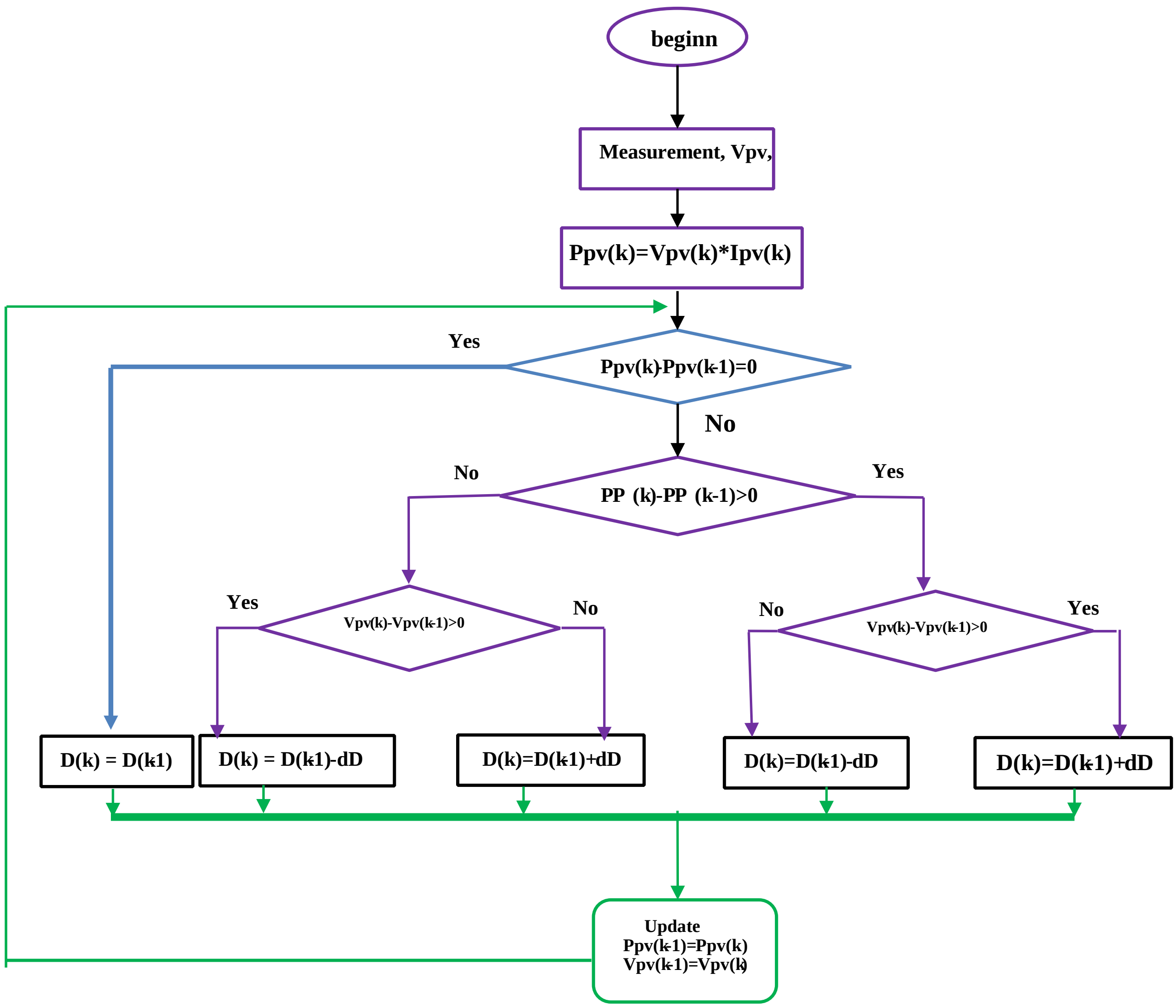

Figure III.5: Flowchart of the P&O algorithm

III.4.2. MPPT algorithms based on fuzzy logic:

Fuzzy logic control has been used in MPPT maximum power point tracking systems; this control offers the advantage of being a robust and relatively simple control to develop and it does not require exact knowledge of the model to be regulated.

The implementation of a fuzzy controller is carried out in three stages, which are: fuzzification, inference and defuzzification.

III.4.2.1. Principle of fuzzy logic:

The general principle and basic theory of fuzzy logic is the description of a phenomenon which generally contains fuzzy expressions such as: Hot, cold. Fast, slow. Large, medium, small. Max, min. Positive, zero, negative…etc.

The elements constituting the basic theory of fuzzy logic are: Linguistic variables, fuzzy sets and membership functions [29].

III.4.2.2. Linguistic variables and fuzzy sets:

The imprecise description of a certain situation, a phenomenon or a physical quantity can only be done by relative or vague expressions, namely; (large, small, positive, negative, etc.). These different classes of fuzzy expressions called fuzzy sets form what we call linguistic variables. Each linguistic variable is characterized by a set such that [30]:

{x, T(x), U, G, M}

Or :

x: is the name of the variable,

T(x): is the set of linguistic values that x can take,

U: is the universe of discourse associated with the basic value,

G: is the syntactic rule to generate the linguistic values of x,

M: is the semantic rule for associating a meaning with each linguistic value.

III.4.2.3. Membership functions:

Each fuzzy subset can be represented by its membership function. In general the shape of membership functions depends on the application, and can be triangular, trapezoidal or bell-shaped as shown in (Figure III.6) [30].

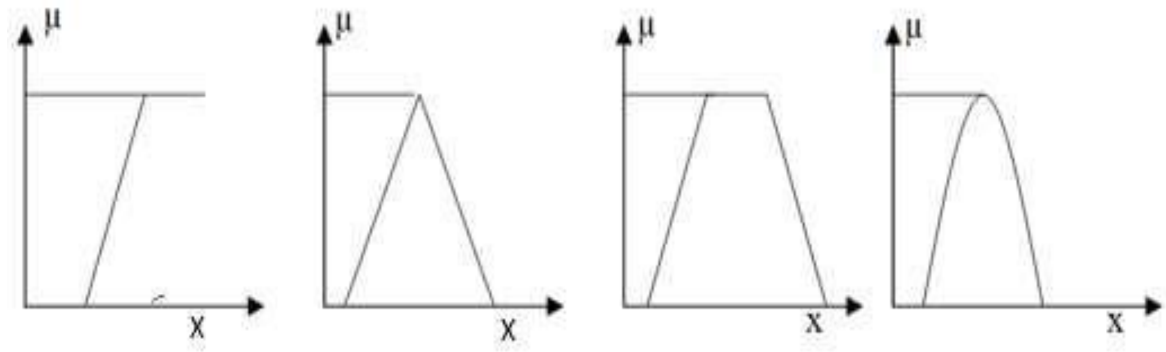

Figure III.6: Different forms of membership functions

III.4.2.4. Linguistic rules:

The main idea of systems based on fuzzy logic is to express human knowledge in the form of linguistic rules of the form If…then…Each rule has two parts [30]:

- Antecedent part (premise or condition), expressed by If…,
- Consequent part (conclusion) expressed by then.

The antecedent part is the description of the state of the system. The consequent part expresses the action that the operator who controls the system must perform. Each fuzzy rule is based on the fuzzy implication. There are several forms of If...then...the general form is:

If (a set of conditions is satisfied) then (a set of consequences can be executed).

III.4.2.5.General structure of a fuzzy system:

The fuzzy logic-based system is composed of four main blocks (Figure III.7).

- Fuzzifier

- Fuzzy knowledge base,
- Engine difference blurred
- Defuzzicator.

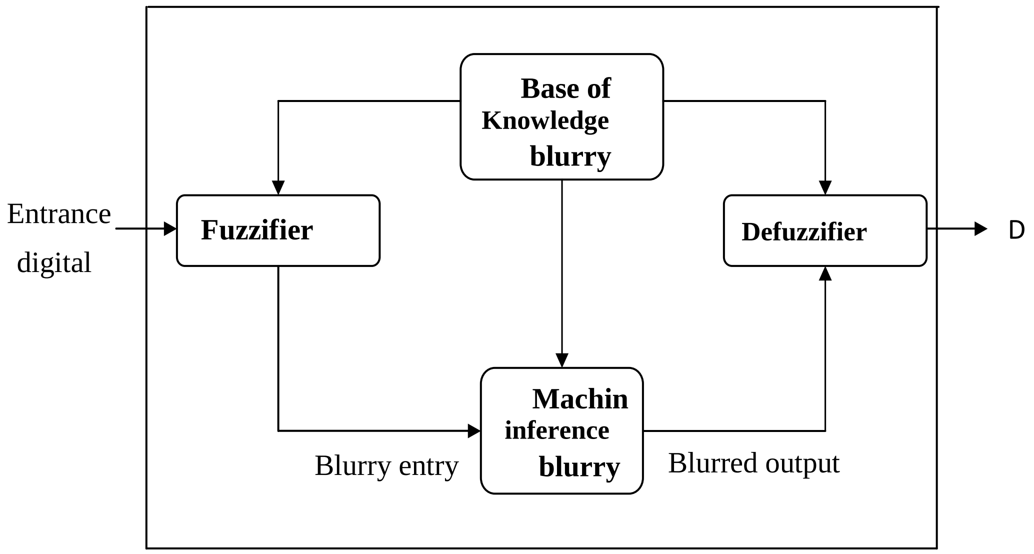

Figure III.7: General structure of a system based on fuzzy logic

III.4.2.5.1. Fuzzification:

The objective of fuzzification is to define the membership functions for the different variables which makes it possible to fuzzy the input variables. A preliminary step consists of defining a maximum variation interval authorized for the input variables. The goal of fuzzification is to transform input variables into linguistic variables or fuzzy variables [29].

Controls are selected depending on the satisfaction of two control variables in the proposed input; they are the E error and the change in CE error in the k-test. We display the E and CE variants in the following form:

$$E(k) = \frac{P(k)-P(k-1)}{V(k)-V(k-1)} \quad \text{(III-4)}$$

$$CE(k) = E(k) - E(k-1) \quad \text{(III-5)}$$

III.4.2.5.2. Knowledge base:

The knowledge base is the heart of the fuzzy control system. This is the basis of inference for fuzzy control. The knowledge base defines all relevant language control rules and settings. The derivation of fuzzy control rules can be performed in four modes. These four modes are not mutually exclusive, and it is necessary to combine them to obtain an efficient system [28].

III.4.2.5.3. Fuzzy inference:

It is mentioned that fuzzy inferences are based on generalized modus ponens fuzzy implication. Inferences link the measured quantities and the output variables using linguistic rules. These rules are combined using the connections and and or. Suppose that the fuzzy system has two inputs x, y and an output z and that we have defined n linguistic rules as follows [31]:

If x=A1 and y=B1 then z=C1

If x=A2 and y=B2 then z=C2

If x=An and y=Bn then z=Cn

Where x, y and z are linguistic variables that represent process state variables and control variables; Ai, Bi and Ci (i=1, n) are the fuzzy subsets defined in the reference sets for x, y and z respectively. In general, any combination of the operators or, and and not can appear in the condition of a rule, depending on the conditions imposed by the system to be adjusted. There are several methods to perform these operators. We therefore introduce the notion of inference methods.

The most used methods are:

- max-min inference method
- max-prod inference method
- sum-prod inference method

In our work, we use the 1st method (max-min inference method).

III.4.2.5.3.1. Max-min inference method:

For this inference method the AND operator is carried out by the formation of the minimum, the OR operator is carried out by the formation of the maximum, and THEN (the implication) is carried out by the formation of the minimum [29].

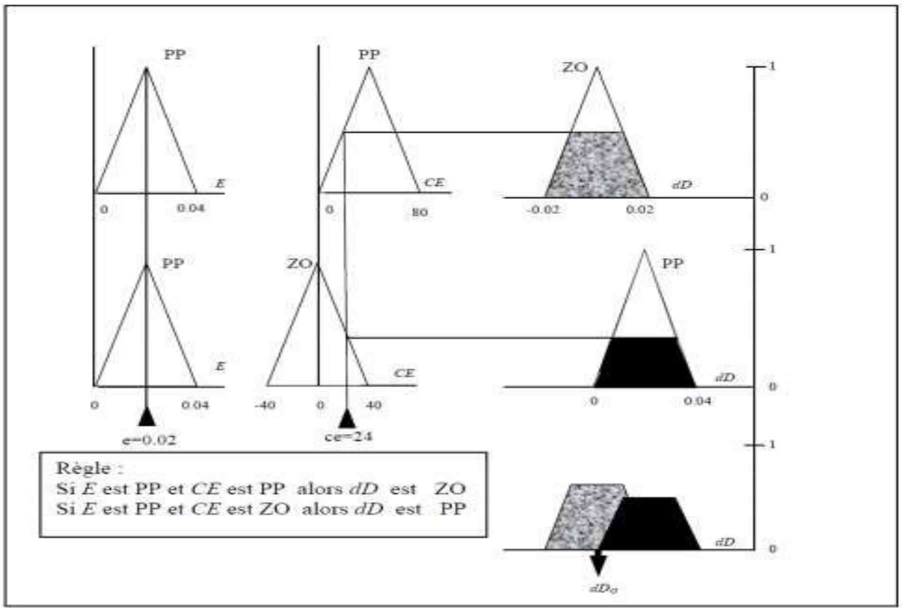

Figure III.8: MAX-MIN composition

III.4.2.5.4. Defuzzification:

The result of a fuzzy inference is a membership function. It's a fuzzy subset. A control device requires a precise control signal. The fuzzy transformation into determined information is defuzzification (concretization). In addition, signal processing and digital/analogue conversion must often be provided. There are several defuzzification methods proposed in the literature. There is no systematic strategy for choosing among any of these methods [30].

There are several fuzzy regulator models such as:

- MAMDANI type fuzzy regulator
- SUGENO type fuzzy regulator
- Fuzzy LARCEN model

- Blurred model of TSUKAMOT

We will explain the MAMDANI type fuzzy regulator

$$\Delta\mathrm{D} = \frac{\sum_{j=1}^{n} \mu(\Delta\mathrm{D}_j).\Delta\mathrm{D}_j}{\sum_{j=1}^{n} \mu(\Delta\mathrm{D}_j)} \qquad \text{(III-6)}$$

the actual duty cycle ratio D is calculated as follows:

$$D(k) = D(k-1) + S_{\Delta\mathrm{D}}\Delta\mathrm{D}(\mathrm{k}) \qquad \text{(III-7)}$$

III.4.2.5.4.1. Mamdani method:

The Mamdani method is the most widely used fuzzy interface strategy. Since it was proposed in 1975, by Professor Ebrahim Mamdani of the University of London who built one of the fuzzy systems to control a combination of steam engine and boiler. In Mamdani's method, a set of fuzzy if-then rules was applied, and these were provided by experienced human operators [28].

Mamdani fuzzy logic uses linguistic variables to describe process states and uses these variables as inputs to control the rules. The terms of linguistic variables are fuzzy sets with a certain shape. Mamdani fuzzy logic usually uses the trapezoidal or triangular fuzzy set, but other shapes are possible.

III.4.2.5.5. The Advantages of Fuzzy Logic:

The main advantages of fuzzy regulators are as follows:

The direct incorporation of fuzzy and linguistic information, coming from a human expert, into the fuzzy system.

There is no need to make a mathematical model of the system to be adjusted.

The fuzzy system is a universal approximator, that is to say, it is general enough to generate any action.

Fuzzy logic is easy to understand by non-experts because it mimics the strategy of human reasoning.

We can master non-linear systems that are difficult to model [30].

III.4.2.5.6. The disadvantages of fuzzy logic:

- Lack of precise guidelines for the design of a regulator,
- Adjustment precision generally low [30].

III.4.3. MPPT algorithm based on fuzzy logic:

To improve the previously proposed fuzzy logic-enhanced P&O MPPT algorithm, we will discuss in the following part the use of MPPT based entirely on the theory of fuzzy logic. The advantage of this method is that it can work with imprecise input values and does not need a high-precision mathematical model. In addition, it can deal with nonlinearities.

In our case, the principle is based on two input variables which are the power Ppv and the current Ipv and an output variable D which represents the duty cycle used to control the static converter to seek the PPM.

This method is effective especially during changing climatic conditions. The following figure shows the basic block diagram of the fuzzy logic based MPPT algorithm.

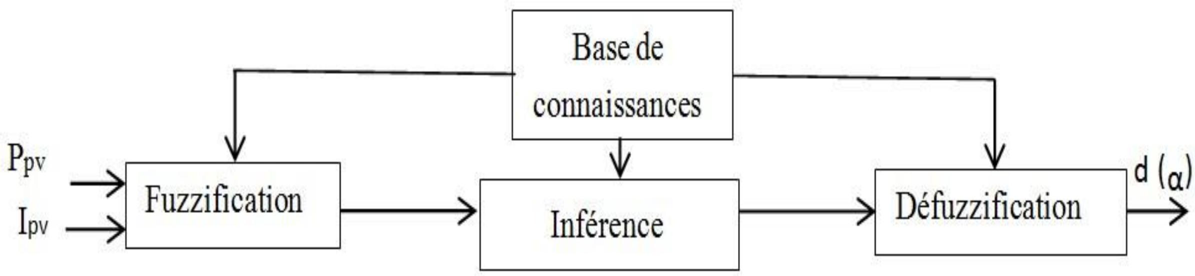

Figure III.9: Block diagram of the MPPT algorithm based on fuzzy logic

In particular, this command is better suited to nonlinear systems. The operation of this algorithm is done in three blocks: fuzzification, inference and defuzzification (Figure III.9) [32].

Fuzzification allows the conversion of physical input variables into fuzzy sets.

The input quantities are assigned the linguistic variables: NG (Negative Large), NM (Negative Medium), NP (Negative Small), Z (Zero), PP (Positive Small), PM (Positive Medium) and PG (Positive Large). The representation of our input variables is shown in the figure (Figure III.10).

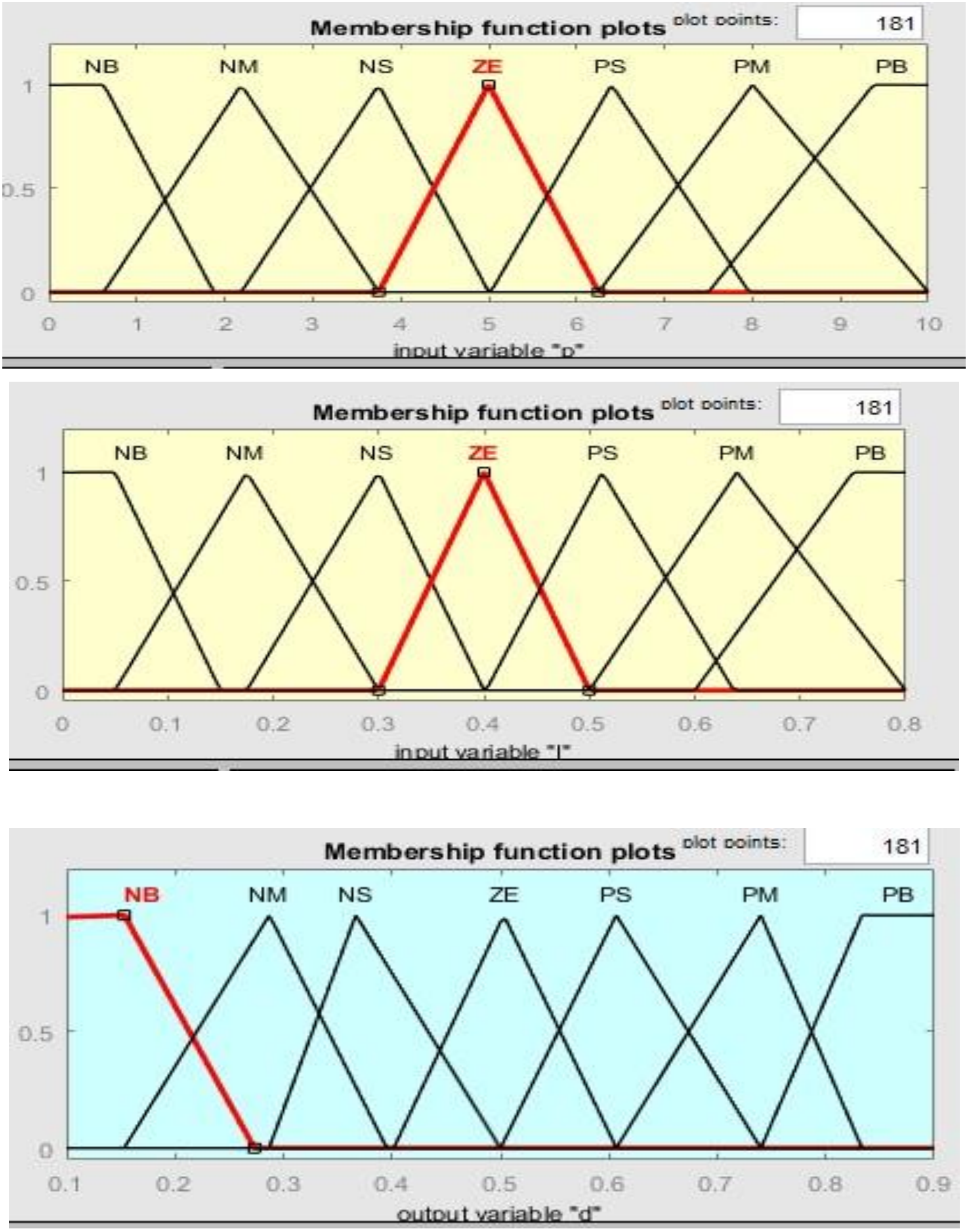

Figure III.10: The subsets for the inputs (a) Ppv, (b) Ipv and the output (c) D

In the inference stage, decisions are made. Indeed, we establish logical relationships between the inputs and the output while defining the membership rules. Subsequently, we draw up the table of inference rules (Table II.2). Finally, in defuzzification, we convert the output fuzzy subsets into a digital value

P/I	**N.G.**	**N.M.**	**NP**	**Z.E.**	**PP**	**PM**	**PG**
N.G.	Z.E.	Z.E.	Z.E.	N.G.	N.G.	N.G.	N.M.
N.M.	Z.E.	Z.E.	Z.E.	NP	N.M.	N.M.	N.M.
NP	NP	Z.E.	Z.E.	Z.E.	NP	NP	NP
Z.E.	N.M.	NP	Z.E.	Z.E.	Z.E.	PP	PM
PP	PP	PM	PM	PP	Z.E.	Z.E.	Z.E.
PM	PM	PM	PM	Z.E.	Z.E.	Z.E.	Z.E.
PG	PG	PG	PG	Z.E.	Z.E.	Z.E.	Z.E.

Table (III 2): Rules of inference

III.5. Conclusion:

In this chapter, we have begun the most important and most delicate part of this study. This is the description of the DC/DC converter which is a power converter (Boost type DC/DC controlled by an MPPT algorithm.

In the first part of this chapter, we presented the principle of the direct connection between the photovoltaic generator and the load. Then, we theoretically studied the operation of a Boost type converter which is used very often. These converters are controlled by varying the duty cycle of the switch control signal which is deduced from the MPPT algorithm.

The second part is devoted to the explanation of the MPP research principle after the study of the different MPPT algorithms used in our work, the disturbance and observation method, the P&O algorithm improved by fuzzy logic, and finally the algorithm MPPT based on fuzzy logic, we were particularly interested in the algorithm based on fuzzy logic which is a robust and efficient algorithm. However, the implementation of these types of algorithms is the objective of the next chapter.

CHAPITRE IV

Results and simulation

IV.1. Introduction

This chapter present how the SIMULINK models of the proposed PV power systems are implemented, to test and verify the functionality of the proposed MPPT controls. In this work, two different MPPT controls implemented in MATLAB/SIMULINK environment. perturb and observe (P&O) algorithm and fuzzy logic control (FLC) with DC-DC boost converter to demonstrate the feasibility and performance of the proposed controller based on MPPT of PV system. Furthermore, a comparison has been carried out between the proposed controllers by way of simulation results.

The presentation of the error, variation of the error and the change in duty cycle is shown in (Figure IV.1).

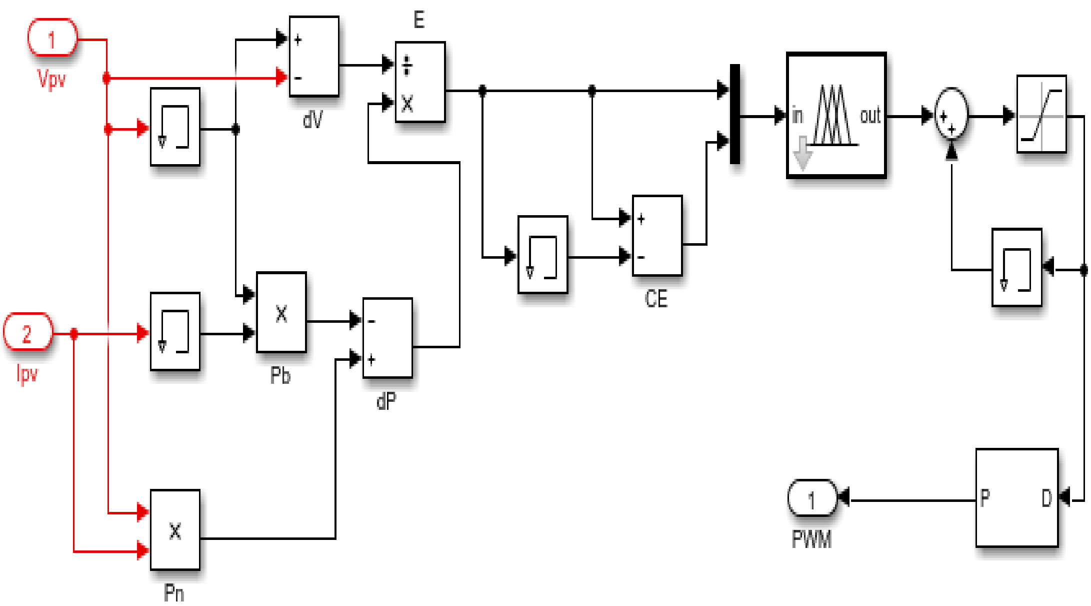

Figure IV.1: Block diagram of fuzzy MPPT algorithm

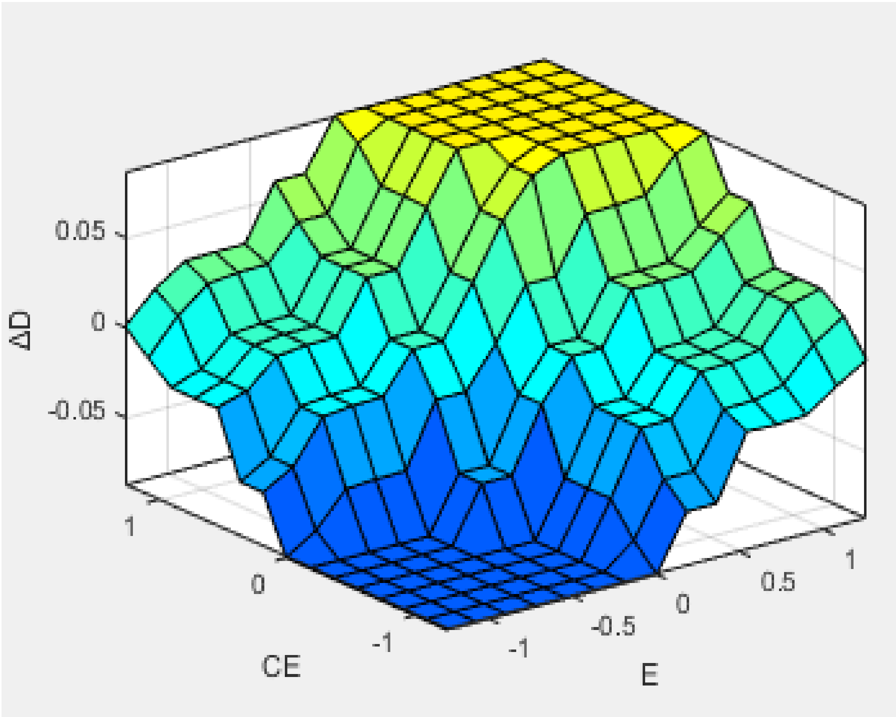

Figure IV.2: 3D presentation of the error, variation of the error andthe change in duty cycle

To study the comparisons of the two algorithms and see the difference betweenvthem, we carried out a test where the two controllers undergo the same standard operating conditions, that is to say constant sunshine equal to 1000 W/m2and a temperature equal to 25°C (figure III.23 and figure III.24).

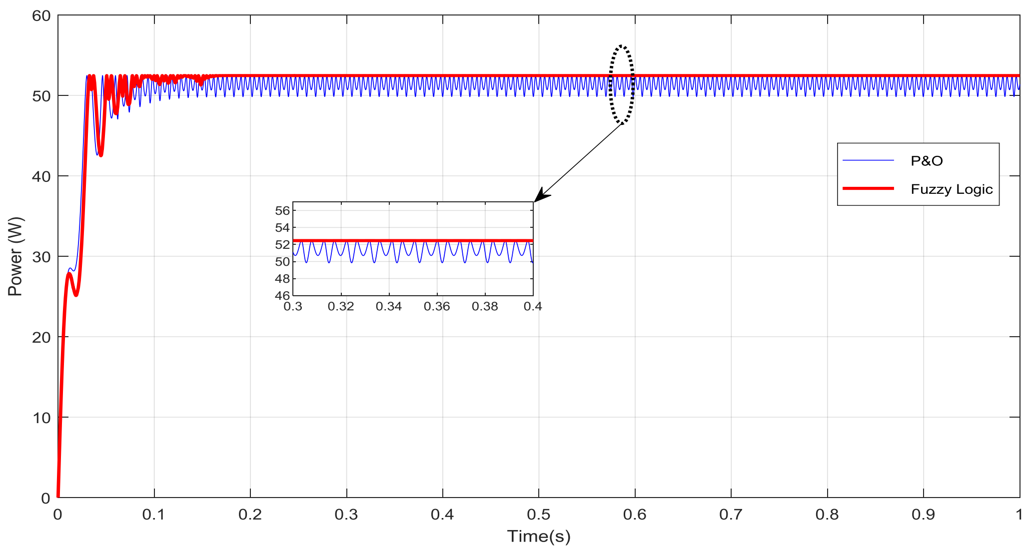

Figure IV.3: Output power of FLC and conventional P&O controller

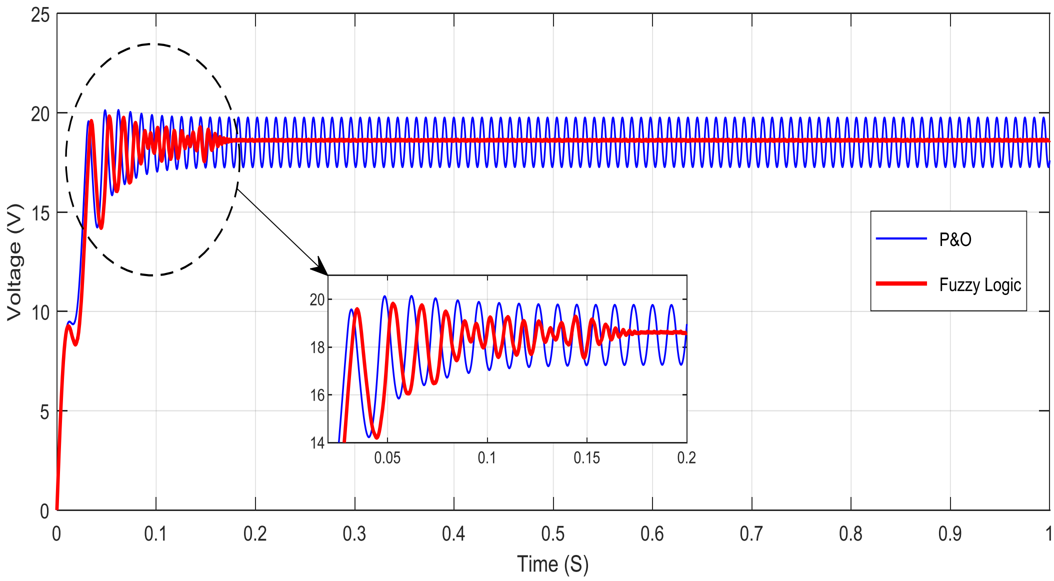

Figure IV.4: Output current of FLC

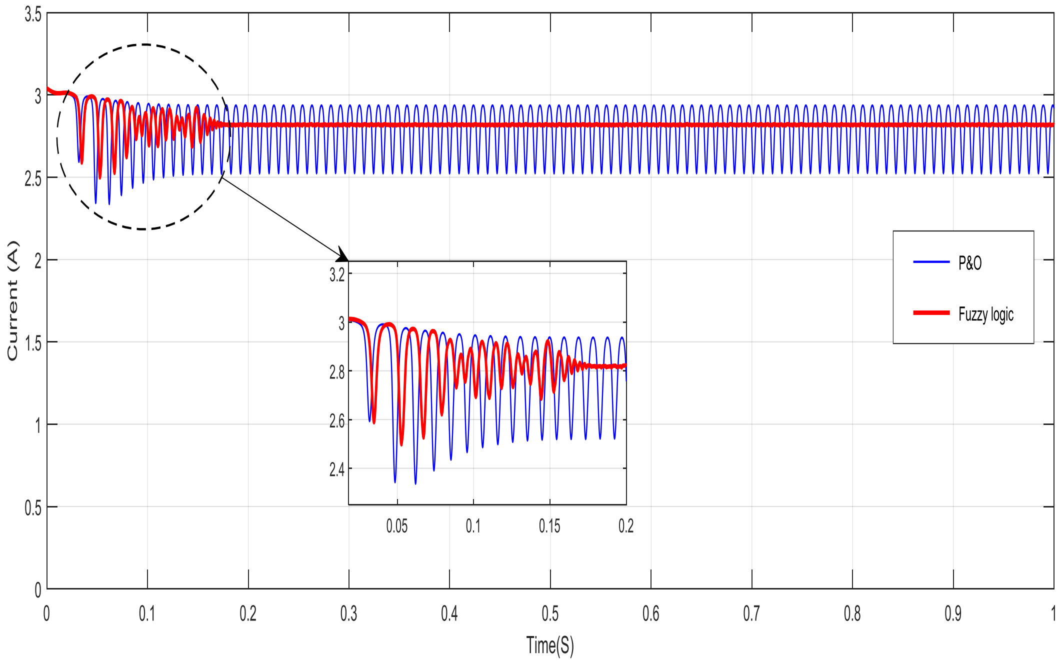

Figure IV.5: Output voltage of the controlled techniques

Figures (III.23, 24) present the power of the photovoltaic generator (Ppv) for the two MPPT control methods (disturbance and observation (P&O) and the fuzzy logic controller (FLC). It can be seen that the method (P&O) presents oscillations around the maximum power point in steady state which induces significant power losses, on the other hand the fuzzy controller makes it possible to reduce power fluctuations in steady state.

IV.2. Robustness test:

To carry out a study of the robustness of the two controllers with respect to the different environmental conditions, we vary the sunshine in both directions of variation: either an increase or a decrease with the maintenance of temperatures at 25°C. This case shows us the behavior of the fuzzy MPPT controller and the fuzzy MPPT PI controller, for a fixed temperature of 25°C and a sudden decrease in sunshine from 800 to 900 W/m2 then an increase from 900 to 1000 W/m2 .

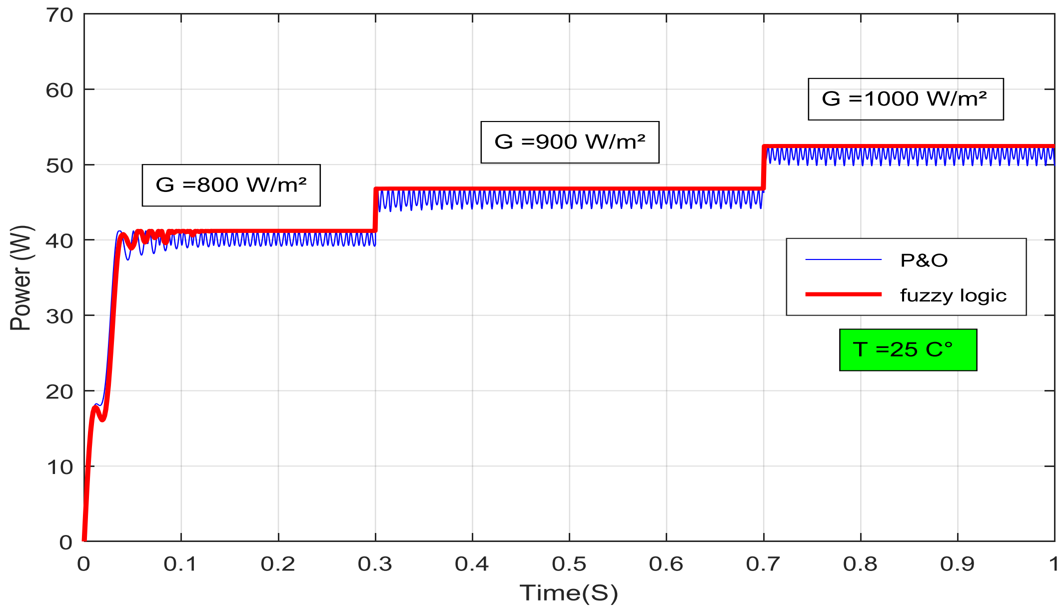

Figure IV.6: Output power of the tested model

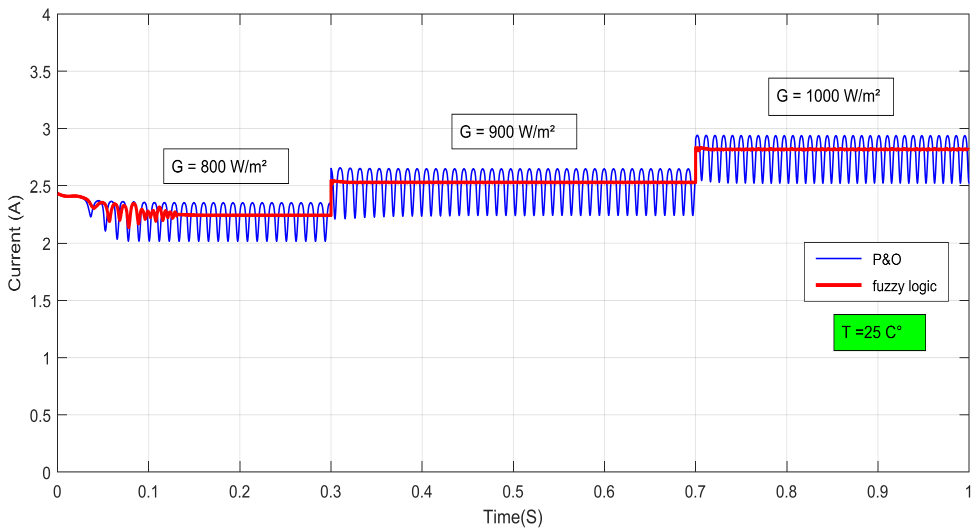

Figure IV.7: Output current of the simulations of the PV panels

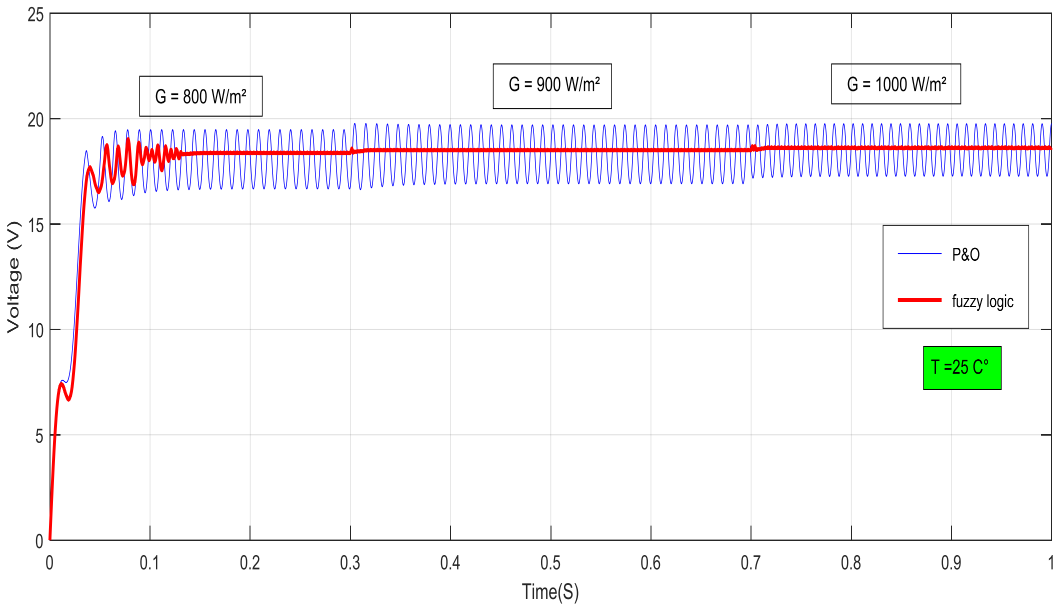

Figure IV.8: voltages at different environmental

According to the robustness test, we see that in the case of a change in sunshine the two commands follow the instructions. Also note that the P&O control takes longer to stabilize on a new PPM, while the fuzzy control stabilizes very quickly This comparative study of the two proposed controls showed that the controller based on fuzzy logic control better optimizes the operating power of the system.

IV.3. Conclusions:

In this chapter, we have started the most important part of this study. This involves presenting the principle of searching for the maximum power point while giving the different classifications of MPPT commands. We have detailed the MPPT disturbance and observation and fuzzy logic methods and made a comparative study between the two we have recalled some notions relating to fuzzy logic necessary to understand the operating principle of a fuzzy regulator. Ultimately, the fuzzy MPPT control performance obtained very good results in terms of response time and efficiency.

Général conclusion

Général conclusion

In conclusion, this comprehensive document serves as a valuable resource for understanding, modeling, and optimizing the performance of photovoltaic (PV) systems. It covers the fundamental principles of solar radiation and the photovoltaic effect that enables the conversion of sunlight into electrical energy using different solar cell technologies.

Accurate equivalent circuit models are presented to analyze the current-voltage behavior of PV cells and generators, taking into account the influence of various parameters such as irradiance, temperature, series resistance, and ideality factors. These modeling techniques provide a strong theoretical foundation for predicting the performance of PV systems under varying environmental conditions.

A significant emphasis is placed on maximum power point tracking (MPPT) algorithms, which are crucial for ensuring that the PV system operates at its maximum power output despite fluctuations in atmospheric conditions. The document evaluates different approaches, including the classical perturb and observe (P&O) method, variants incorporating fuzzy logic for improved tracking performance, and a completely fuzzy logic-based MPPT controller.

The analysis and modeling techniques, coupled with the MPPT algorithms studied in this document, offer practical solutions for designing and optimizing photovoltaic systems. By implementing the proposed methods, researchers, engineers, and practitioners can significantly improve the energy conversion efficiency from solar radiation to electrical power output, ensuring continuous operation at the maximum power point under all environmental conditions.

Bibliographic références

Bibliographic références

[1] Soltane. Belakehal « Conception & Commande des Machines à Aimants Permanents Dédiées aux Energies Renouvelables ». Thèse de doctorat, Université de Constantine, 2010.

[2] Cabal. Cédric « Optimisation énergétique de l'étage d'adaptation électronique dédié à la conversion photovoltaïque ». Thèse de doctorat, Université de Toulouse, 2008.

[3] Roshanak. Radbeh « Réalisation et caractérisation des cellules solaires organiques à Couches composites polymères incluant des nanotubes de carbones ». Thèse de doctorat, Université de Limoges, 2008.

[4] Alonso Corinne « Contribution à l'optimisation, la gestion et le traitement de l'énergie ». Mémoire d'habilitation à diriger les recherches, Université Paul Sabatier Toulouse III, 2003.

[5] Thibaut Desrues, « Développement de cellules photovoltaïques à hétéro jonctions silicium et contacts en face arrière ». Thèse de doctorat, L'institut national des sciences appliquées de Lyon, 2009.

[6] Petibon Stéphane « Nouvelles architectures distribuées de gestion et de conversion de l'énergie pour les applications photovoltaïques ». Thèse de doctorat, Université de Toulouse, 2009.

[7] José Miguel Navarro « Cellules Photovoltaïques Organiques Transparentes Dans Le Visible ». Thèse de doctorat. Université Toulouse III - Paul Sabatier, 2008.

[8] Benis Halouma « Contribution à la modélisation du problème de Hot Spot dans les modules solaires Photovoltaïque occultées ». Mémoire de magister en électrotechnique, Université Mentouri de Constantine, 2008.

[9][12] Souad. Saadi « Effet des paramètres opérationnels sur les performances d'un capteur solaire plan ». Mémoire de magister en Physique, Université Mentouri de Constantine, 2010.

[10] Bouden. Abdmalek « Analyse optimisée de système de pompage photovoltaïque ». Mémoire de magister en électrotechnique, Université Mentouri de Constantine, 2008.

[11] Amina Benhammou « Optimisation d'un nouveau système de séchage solaire modulaire pour plantes aromatiques et médicinales ». Thèse de doctorat, Université de Abou Bekr Belkaid Tlemcen, 2010.

[13] BOUKLI-HACENE Omar, « Conception et Réalisation d'un Générateur Photovoltaïque Muni d'un Convertisseur MPPT pour une Meilleure Gestion Energétique », Thèse de Magister, Université Abou Bakr Belkaid de Tlemcen (Décembre 2011).

[14] ZERROUKI Zolikha et BEREKSI REGUIG Rym « Dimensionnement d'un système photovoltaïque autonome », Mémoire de master, Université Abou Bakr Belkaid de Tlemcen (2016 / 2017).

[15] BOUKHERS Djamila « Optimisation d'un système d'énergie photovoltaïque Application a pompage », Mémoire de Magister, Université Mentouri de Constantine (28/ 11/ 2007).

[16] Angel Cid Pastor « Conception et réalisation de modules photovoltaïques électroniques », thèse de doctorat. Institut National Des Sciences Appliquées de Toulouse, 2006.

Bibliographic références

[17] C. Lerouge « Recherche & Industrie Photovoltaïque (PV) Etats-Unis » Sciences physique États-Unis, 2006.

[18] Helali Kamelia « Modélisation d'une cellule photovoltaïque: Etude comparative », Mémoire de magister, département d'électrotechnique, faculté du génie électrique, UMMTO 2012.

[19] Charly Cornu « Centrales photovoltaïques (Guide pour le dimensionnement et la réalisation de projets A l'usage des bureaux d'ingénieurs) », office fédéral des questions conjoncturelles, 1996.

[20] M. Kenane, S. Sadoudi « Modélisation de modules photovoltaïques en milieu réel d'implantation », Mémoire de Master II, département de génie mécanique, faculté du génie de la construction, UMMTO 2013.

[21] Y. JAUTARD, T. BOUDOL, L'électricité photovoltaïque, Site Internet "Architecture et énergies renouvelables", 2000.

[22] Anne, Labouret, Michel, Villoz., Energie photovoltaı¨que. (Dunod 3e`me e´dition 2006).Bernard Equer, Energie solaire photovoltaı¨que (Ellipses 2004).

[23] N. Abouchabana, « Etude d'une nouvelle topologie buck-boost appliquée à un MPPT », Mémoire de Magistère, Ecole Nationale Polytechnique, Alger, Algérie, 2009

[24] C.Galize, « Introduction à l'électrotechnique et à l'électronique de puissance » Cours, Université de Montpellier II, 2002.

[25] M.Boukli-Hacene Omar, « Conception et Réalisation d'un Générateure Photovoltaique Muni d'un Convertisseur MPPT pour une Meilleure Gestion Energétique »,These de Magister, Universite Abou Bakr Belkaid-Tlemcen, 2010.

[26] A. Ahmed Azi, « Contribution au développement d'un outil d'aide au diagnostic de performances des MPPT dans la chaine de conversion photovoltaïque » Mémoire Master Universite Kasdi Merbah, Ouargla, 2016.

[27] Fathi A O Aashoor « Maximum power point tracking techniques for photovoltaic water pumping system » Doctor thesis of Philosophy, University of Bath, May 2015.

[28] Messaoudi Mohammed Tahar « Simulation d'un système photovoltaïque autonome régulé par logique floue ». Mémoire Master , Universite Kasdi Merbah Ouargla. 2015.

[29] Mohamed Redha Rezoug, Rachid Chenni and Djamel Taibi « Fuzzy Logic-Based Perturb and Observe Algorithm with Variable Steps of a Reference Voltage for Solar Permanent Magnet Synchronouns Motor Drive System Fed by Direct-Connected Photovoltaic Arry » Renew. Energies, 2018, 11, 02–15

[30] :H. Abbes , H. Abid , K. Loukil , A. Toumi et M. Abid « Etude comparative de cinq algorithmes de commande MPPT pour un système photovoltaïque ». National School of Engineering of Sfax, University of Sfax. Septembre 2014.

[31]: BOUKHERS Djamil « optimisation d’un système d’énergie ph otovoltaïque application au pompage » Memoire Magister, Université Mentouri de Constantine, 2007.

[32] http://www.technologuepro.com/cours-circuits-numeriques/Chapitre4%20CN.pdf.